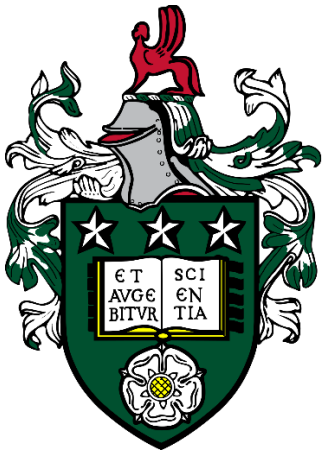

DEVELOPMENT OF OPTIMISATION SCHEMES FOR ULTRASOUND PARTICLE SIZING AND CONCENTRATION MEASUREMENTS

BINGQIAN XU

Submitted in accordance with the requirements for the degree of

Master of Philosophy

The University of Leeds

School of Chemical and Process Engineering

September 2023

DECLARATION

I confirm that the work submitted is my own and that appropriate credit has been given where reference has been made to the work of others. The initial idea (especially the novel, simultaneous determination of material properties and particle size distribution parameters through optimisation), how it should it work, how data should be obtained and analysed are all mine, my supervisor only helped with software implementation.

ACKNOWLEDGEMENTS

I sincerely thank my supervisors, Dr. Xiaodong Jia and Professor Xue Wang, for their assistance, guidance, and encouragement throughout the past several years. Without your support, it would have been impossible to complete much of the research in this thesis. I am grateful to my colleagues and teachers at the laboratory in Guangzhou for their help and valuable discussions.

Lastly, and most importantly, I express my gratitude to my family for their encouragement and financial support, which allowed me to complete this degree.

ABSTRACT

Particle size is a critical indicator of product quality, significantly affecting product stability, solubility, and flowability. With the advancement of science and technology and the improvement of industrial standards, particle size measurement has become increasingly important in many fields, such as chemical engineering, pharmaceuticals, and materials science. Among the numerous particle size distribution measurement techniques, ultrasonic attenuation spectroscopy has attracted the attention of many researchers due to its strong penetration ability, wide frequency range, fast response speed, and non-contact advantages. The most classic theoretical model in ultrasonic attenuation is the ECAH model, which is widely applicable because it covers most comprehensively the attenuation mechanisms. However, a major limitation of the ECAH model is that it requires many material properties parameters, many of which are unknown or inaccurate. Given some test run results, it is possible to use a retrofitting process to determine what those unknown/inaccurate values should be to minimise the error between the measured and ECAH predicted results. The aim of this project is to compare error minimisation algorithms and evaluate how they perform in different scenarios. The main novelty of the research is that both unknown/inaccurate material properties and particle size distribution (PSD) parameters can be determined simultaneously through an optimisation process. The tested optimisation algorithms include Genetic Algorithm (GA) optimisation, Particle Swarm (PS) optimisation and Parallel Traversal (PT) algorithm.

This research will have a significant impact on the field of ultrasonic attenuation spectroscopy for PSD measurement. Firstly, for the first time, a systematic sensitivity analysis has performed for all the optimisable parameters. This is useful in narrowing the range of values a parameter can have when it is being optimised, thus helping to

speed up the optimisation process. Secondly, the simultaneous optimisation of both material properties and PSD parameters has been shown to give more accurate result than optimising parameters and PSD separately. Finally, test results have indicated that if the number of parameters to be optimised is small (e.g., <=3), PT is the quickest among the three for comparable setups; for more parameters, GA runtime is more predictable than PS.

TABLE OF CONTENTS

LIST OF FIGURES

LIST OF TABLES

CHAPTER 1. INTRODUCTION

1.1 Problem Statement and Motivation

Crystallisation is a separation process which widely used for product purification in many industries. In the pharmaceutical industry, crystallisation is used to obtain crystalline APIs (active pharmaceutical ingredients) with satisfactory size, shape, crystalline form, and chemically pure substances, because these properties affect the bioavailability and stability of the API.

Crystallisation of a chemical in a solution often involves two steps: nucleation and growth. The crystal nucleus is also the particle. There are many issues related to particles in industrial production, pharmaceutical and environmental protection. Usually, particles refer to small, dispersed objects, which can be solid, liquid or gas. In our daily life, we may contact various kinds of particles inevitably, which play a very important role in the survival and development of human beings. At present, the research on particles has been deeply carried out in all walks of life (Peter, 1996). It is proved that the size and nature of the particles control the quality and performance of products and materials in many production processes, which affect energy consumption and people's health (Coston and George, 1991). It has been pointed out that in the chemical and pharmaceutical industries, more than 60% of products (including intermediate products) are in the form of granules or powders, and about 20% of them are closely related to the quality and performance of the particles. In addition, in the food industry, the size of the various particles produced during the food production process has a significant impact on the physicochemical properties of the emulsification, suspension and foam dispersion systems, which to some extent determines the stability, appearance and Taste, etc. (Sullo and Norton, 2016, Dickinson et al., 1994). The performance of light industrial products such as photographic film, ceramics, toothpaste,

etc. is also inseparable from the particle size. Another example like the suspension of pollutants in soot, natural gas or industrial wastewater from atmospheric or industrial waste gas. If it is not properly measured and treated, it will cause great harm to people's health (Yu and Standish, 1990).

The particle size is not strictly limited, and in many cases, it refers to particles having a particle diameter of 1000μm or less. In recent years, with the rapid development of micro-nano technology, sub-micron and nano-particles with surface effects, volume effects and quantum size effects have exhibited various characteristics such as light, electricity and heat, and are widely used in various fields (Henggao and Rong, 2007). Therefore, people have put forward higher requirements for particle detection technology.

From the above, it is clear that the size and size distribution of the particles determine the quality and performance of the product in industrial processes and many applications. Undoubtedly, accurate measurement of particle size and particle size distribution has significant economic and social meaning for improving product quality, accelerating technological development, controlling environmental pollution, and safeguarding human health (Coston and George, 1991).

In this research, the focus is on measuring particle size distribution (PSD), PSD measurement is the most basic and important part of particle measurement. There are many methods for measuring particle size. As early as the 1980s, there were more than 400 kinds of particle measuring instruments already (Ziemann and McMurry, 1998). Depending on the measurement principle, the measurement methods can be divided into the following categories: light scattering, microscopy, sieving, sedimentation, and ultrasonic attenuation spectroscopy (Zelenyuk et al., 1999, Hui et al., 2014, Wen-kai et al., 2007). These methods have their own characteristics and application range. Among

them, ultrasonic attenuation spectrum (UAS) method as a relatively new type of measurement method, has attracted more and more attention.

UAS measurement of the PSD of particles in a suspension depends on the propagation of sound waves. it's intensity changes when sound waves penetrate the suspension. The size information of the particles is obtained by measuring the attenuation of the ultrasonic waves passing through the tested sample. Due to the wide frequency of ultrasonic waves, the particle size can be measured in the range of 20 nm to 1000 μm. One of its advantages is that it can be used for the measurement of particle size in high solid concentration up to 50 vol% suspensions and emulsions. There are many mathematical models for the propagation of ultrasound in the scattering phase system, and different mechanism models are applicable to different systems. Among them, the most concerned is the ECAH model (Spelt et al., 1999, Dukhin, 2002, Shukla et al., 2010). The ECAH model uses the mass, energy, and momentum conservation equations to describe the relationship between acoustic wave propagation velocity, attenuation coefficient, particle size distribution, and concentration.

1.2 Objective of Research

Based on the features of the UAS method in measuring the size of particles as mentioned above, this study aims to validate and develop the accessibility and accuracy of the Nano Sonic ultrasonic particle size measurement instrument. The main objective of this research is to use mathematical optimisation algorithms to simulate and optimise the unknown physical property parameters and simultaneously optimise the particle size distribution results.

1.3 Thesis Structure

Chapter 1 begins by introducing the research background and significance of this thesis. And the research objectives of this thesis are presented.

Chapter 2 provides a comprehensive review of the widely used particle measurement methods both domestically and internationally, as well as the research progress in the field of particle measurement using the UAS method. These studies lay the theoretical foundation for the subsequent experimental research.

Chapter 3 covers the principles of ultrasound, ultrasonic attenuation, and the calculation of models. It also discusses the development and utilization of the hardware and software for the ultrasonic particle size measurement instrument.

Chapter 4 provides an introduction to the mathematical optimisation algorithms and principles used in this study.

Chapter 5 presents the specific mathematical optimisation results based on data obtained from ultrasonic attenuation measurements. This includes sensitivity testing, multi-parameter optimisation, particle size distribution optimisation, and combined optimisation.

The last chapter is conclusion and recommendations for the thesis.

CHAPTER 2. LITERATURE REVIEW

Due to the initial focus of this research on measurement of nucleation process, this chapter includes a section on nucleation theory research. The particle size distribution measurement techniques are the main content of this chapter.

2.1 Particle

In general, particles refer to gas particles, liquid particles, and solid particles, and vital bacteria and microorganisms can also be counted as particles. In certain cases, liquid particles are referred to as droplets, and gas particles are referred to as bubbles, in which case the particles are referred to as solid particles. Particle-related problems are widespread in all aspects of industrial production, daily life and scientific research. There is no strict limit to the particle size, and in most cases the particle size does not exceed a few hundred microns, and in few cases exceeds 1000 μm. The size of the particle has great significance in many areas, such as product quality and performance, environmental pollution problems, human health problems, energy consumption problems, coal-water slurry and pneumatic pipeline transportation, food taste and Shelf life. In the pharmaceutical industry, the size of the particle will affect the body's absorption of drugs, thereby affecting the efficacy. Thus, it can be seen that particle size problems are affecting human life significantly, so it is crucial to find a fast and effective technology to measure particle size.

2.2 Crystal Nucleation Theory

During the process of crystallisation, there are two main steps: nucleation and growth. Nucleation is the foundation of crystallisation; it decides crystal performance

significantly. There are two theories describe the nucleation process. Classical nucleation theory and Two-step nucleation theory.

2.2.1 Classical Nucleation Theory (CNT)

Classical nucleation theory (Corzo et al., 2014, Kim and Karrila, 1991, Myerson and Ginde, 2002) separates nucleation into two parts, primary nucleation, and secondary nucleation. Primary nucleation is the process of unseeded nucleation of solute in solution, it separates into primary homogeneous nucleation and primary heterogeneous nucleation. Primary homogeneous nucleation happened in highly saturated and completely pure solution. Primary heterogeneous nucleation happens in solution which is influenced by dust or other particulate matter. Secondary nucleation happens because there is microcrystal involved in the process of nucleation.

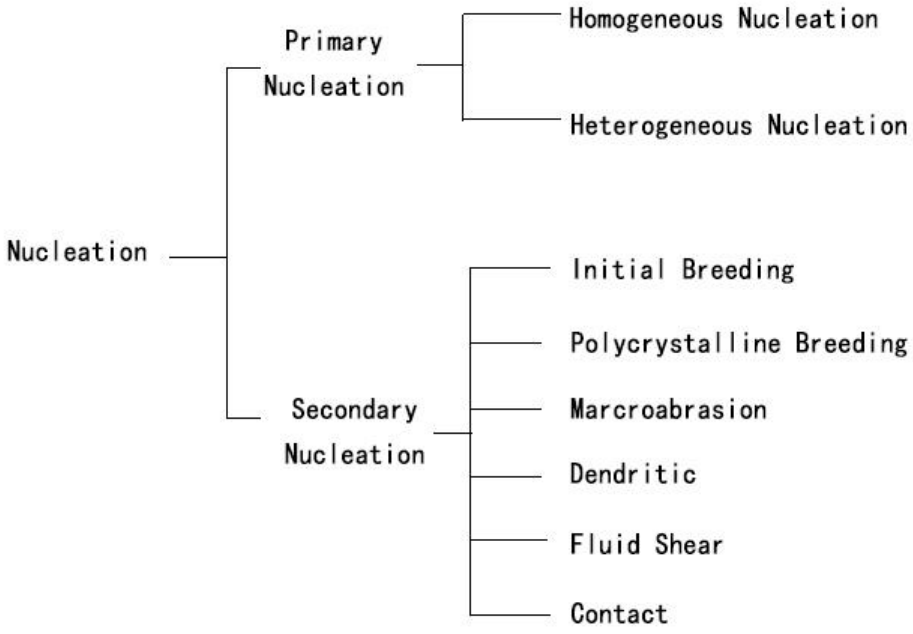

Figure 2.1 Nucleation Classification

The classical nucleation theory is the most widely used nucleation theory. At the tail

end of the nineteenth century, Gibbs (Gibbs, 1879) described nucleation process thermodynamically. He defined the free energy which from the nucleus(ΔG) as the summation of surface free energy (ΔGs) and bulk free energy(ΔGv).

$$\Delta G = \Delta Gs + \Delta Gv \tag{2.1}$$

Nucleation in solution is the process of generating a new solid phase. The following condition is needed for an unseeded nucleation system: ΔG<0(ΔGv <0, ΔGs>0), Figure2.2. Therefore, the nucleation depends on the interplay of ΔGv and ΔGs to decide ΔG in the solution system.

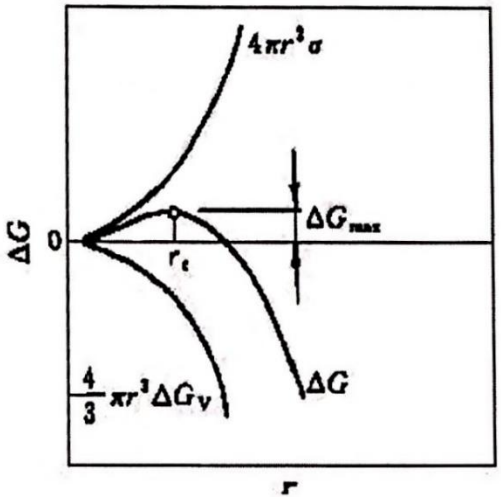

Figure 2.2 The free energy change of nucleation (Gibbs, 1879)

Assume the shape of nucleus is spherical, radius is r,

$$\Delta G_V = \frac{4}{3}(\pi r^3 \Delta G_V) \tag{2.2}$$

$$\Delta G_s = \gamma \Delta A = 4\pi r^2 \gamma \tag{2.3}$$

$$\Delta G = 4\pi r^2 \left(\gamma + \frac{r}{3}\Delta G_v\right) \tag{2.4}$$

When $\frac{d(\Delta G)}{d\gamma} = 0$, Critical radius

$$r_c = \frac{2\gamma V_m}{RT\ ln\, S} \tag{2.5}$$

Critical free energy

$$\Delta G_c = \frac{16\pi\gamma^3 V_m^2}{3(RT\ ln\, S)^2} \tag{2.6}$$

Where γ is Surface tension of solidity-liquid interface

Vm is Molecular volume.

S is Supersaturation

Based on Gibbs explanation of the nucleation process from thermodynamics, researchers define nucleation (J) as number of generated nucleus in the solution at unit time per unit volume, and use Arrhenius equation to describe nucleation rate:

$$J = A\, exp\left(-\frac{\Delta G_C}{kT}\right) = A\, exp\left(\frac{-16\pi\gamma^3 V_m^2}{3k^3T^3(ln\, S)^2}\right) \tag{2.7}$$

In this equation, A means pre-exponential factor, theoretical value is about 1030cm-3s-1, k is Boltzmann's constant.

The nucleation process has been described by classical nucleation theory of thermodynamics and kinetics for quite a long time and established a link between microcosmic molecules level and macro level of the crystal during the nucleation process. From the macro level, the nucleation begins from the sudden change of solution concentration (Drenth and Haas, 1998). From the micro level, the nucleation begins because of the difference of free energy between molecular clusters (Oxtoby, 1992). The Classical nucleation theory can explain most of crystal nucleation

phenomenon, it provided theory and evidence to nucleation and crystal structural analysis (Garcıa-Ruiz, 2003). But hypotheses exist while using the theory describing nucleation process, which make the theory limited: In classical nucleation theory, nucleus cluster is assumed as spherical droplet which internal density uniformly. The density of droplet is same as crystal macro density, and its unrelated to the scale of the droplets (Erdemir et al., 2009). The growth unit sequence of solution is orderly during the nucleation and growth process. The sequence of growth unit in the unit cell and post-growth are same. The solidity-liquid interface tension has no relevance to the scale of nucleus (Laaksonen and Napari, 2001), and solidity-liquid interface energy has no relevance to the temperature of solution neither (Fokin and Zanotto, 2000).The aggregates are assumed constitute by single molecules during the process of nucleation, multiple molecules aggregation is not considered, the possibility of aggregation dissociate are also ignored. As soon as the solution becomes saturated, the solute molecule of the solution will aggregate immediately, and nucleation duration does not affect nucleation rate, the whole nucleation process is steady-state kinetics process.

To sum up, the classical nucleation theory can be used to calculate nucleation rate and critical nucleation radius, but cannot get the route of solute molecule aggregated and inner structure of the nucleus. Moreover, other middle construction may be generated during the nucleate process. There for Two-step nucleation theory is raised in the further study.

2.2.2 Two-step Nucleation Theory

During the study of protein nucleation mechanism, two-step nucleation theory (TNT) was investigated (Vekilov, 2010b, Christenson, 2013). The theory considered the basis of the change in solution structure is the fluctuation of the solution density. After the structure changed, many irregular molecules clusters like droplets are generated, which have an amorphous structure. Then it will Subsequently, it will be rearranged into

ordered clusters of droplet-like molecules, and finally a high density critical metastable region. It may happen in most of the nucleation processes. The Fig.2.3 is the schematic illustration of the classical nucleation theory and the two-step nucleation theory. The two-step nucleation theory can be understood as solute molecules in the solution first aggregate as unordered clusters, the cluster may monomers, dimers, trimers, or polymers. After clusters reached up to a certain extent, its interior will reorder as ordered nucleate, and finally grow into the crystal.

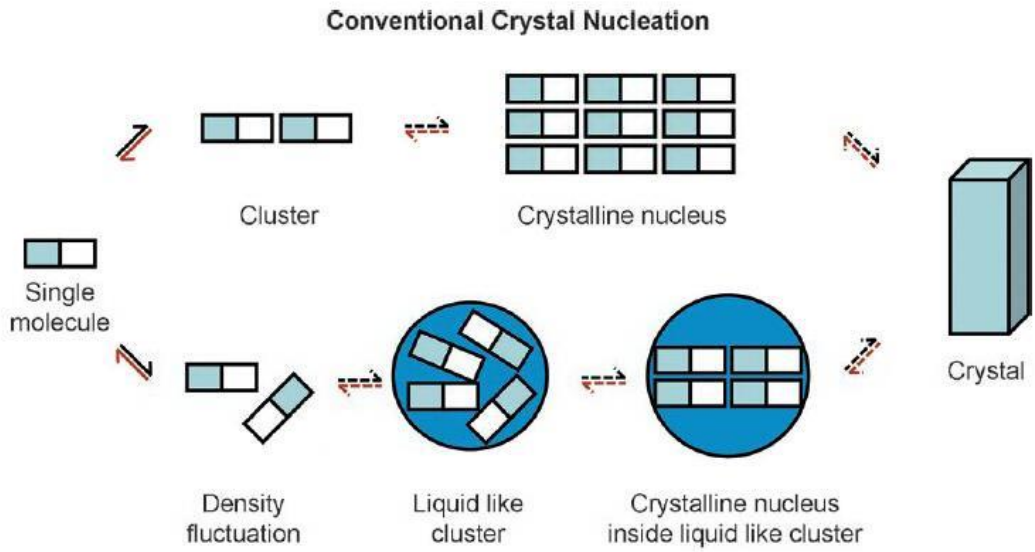

Figure 2.3 The Schematic illustration of Classical nucleation theory and two-step nucleation theory(Davey et al., 2013)

Vekilov (Vekilov, 2005, Vekilov, 2004, Vekilov, 2010a). Made a huge contribution to the development of the two-step nucleation theory. They verified that droplet could be the core of nucleation, it is very useful to study of deoxygenated haemoglobin vulcanized polymer nucleation (Christenson, 2013, Vekilov, 2005).They also explained the nucleation process of lumazine synthetase is unstable clusters on sub - micron level. Meanwhile, it explained that scale of clusters in the solution is not dependent on the

thermodynamic factor, but depend on nucleation and growth kinetics. During the nucleate process, the cluster inside a droplet can arrange as the surface of crystal in a certain time, then the free energy of this nucleus will reduce, to continue the nucleate in process (Gliko et al., 2005, Gliko et al., 2007). They also apply dynamic light scattering and confocal depolarised dynamic light scattering (CDDLS), to study the clusters changing process in nucleation (Maes et al., 2015).

Two-step nucleation theory starts from the study of the nucleation process of macromolecule protein, and the theory concentrates study on molecule clusters in solution before nucleation. Therefore, the change of molecule clusters in solution before nucleation and its correlation between nucleus formation, has become research hotspot. The theory and practice have demonstrated two-step nucleation theory can be used not only in biomacromolecule (like protein and cluster) and colloid system, but also in research of organic small molecules (Kuznetsov et al., 2001, Savage and Dinsmore, 2009, Krishnan and Lindquist, 2005). At present, although many verifications of molecule clusters in solution before nucleation have done, many of them are indirect proof or research with molecular modelling. Thus, there are still many problems to be solved.

2.2.3 Advances in the study of nucleation processes

In 1878， Gibbs (Gibbs, 1879) during the course of studying the thermodynamics of a material system, he first put forward the nucleation theory in the course of studying the thermodynamics of a material system, which was the seed of the classical nucleation theory. He proposed two different types of phase transition processes, one with large variations in degrees and small variations in ranges, and the other with small variations in degrees, known as nucleation. On the basis of Gibbs 'findings, Becker and Doring (Langer, 1968) established the homogenous nucleation theory in the study of the condensation of saturated steam into droplets. For a long time, the theory of

homogeneous nucleation has been used by scientific researchers to analyse the crystallisation process and become the theoretical basis for studying the nucleation process. In 1968, Turnbull et al. (Langer, 1968, Turnbull, 1950). concluded the formula of the homogenous nucleation rate of the crystallisation process, and then put forward the idea of heterogenous nucleation. By comparing the homogenous nucleation with heterogenous nucleation, it is concluded that the resistance of the heterogenous nucleation process is less, the nucleation is easier. The nucleation mechanism of protein was systematically studied by Kam (Kam et al., 1978) and Rosenbergen et al. (Rosenberger et al., 1996), and the nucleation theory was further supplemented and improved to promote the development of classical nucleation theory. Lothe and Pound (Lothe and Pound, 1962) had measured the critical supersaturation of crystal nucleation by experiment, and compared with the calculated value of classical nucleation theory, it was found that the prediction of classical nucleation theory was reasonable when the size of critical crystal nucleus is 16-20 atoms. In this paper, the classical nucleation theory is modified to a certain extent (Hickey and L'Heureux, 2013). Joseph et al. (Hickey and L'Heureux, 2013) had modified the classical nucleation theory's assumption that the surface tension of spherical droplets was constant.

In the course of studying the nucleation mechanism of protein crystallisation process, as the two-step nucleation theory was put forward and developed. Vekilov et al (Vekilov, 2010b, Christenson, 2013, Vekilov, 2005) have conducted a series of experimental studies on the crystallisation process of protein, and put forward and improved the two-step nucleation theory gradually: through the study of nucleation kinetics of lysozyme protein, the application scope of this theory is summarised, and it is pointed out that the nucleation theory is also applicable to organic small molecular matter, polymer, colloid and biological mineral. It is especially suitable for the nucleation of globular proteins and colloids. Wolde and Frenkel (ten Wolde and Frenkel, 1997) used Monte Carlo computer simulation method for the first time, and found the basis of supporting two-

step nucleation theory. They used Monte Carlo technology to study homogeneous nucleation of Lennard-Jones system, which showed that when the solution deviates from the critical point of solution, The density and structure of the solution change at the same time, which is very similar to the description of classical nucleation theory. In the end, it will affect the nucleation process. That is, after the formation of disordered droplets, the interior of droplets larger than the critical size rearranges, and then the crystal nucleus. Gavezzotti et al. (Gavezzotti, 1999) have established a molecular dynamics model containing 50 acetic acid molecules and 1659 CCl4 molecules. When the solvent molecules in the system are removed, the solute concentration becomes larger, forming droplets of solute micelles. The initial stage of crystal nucleation is the formation of microemulsions containing this micelle. To a large extent, molecular dynamics simulation also provides evidence for two-step nucleation theory. Talanquer and others apply density functional theory to the study of crystal nucleation. The rationality of the two-step nucleation theory is further confirmed.

With the continuous development of scientific instrument and equipment, the research on nucleation process has changed from the initial theoretical research to the visual exploration stage. Atomic force microscopy (AFM) is widely used in nucleation research. Atomic force microscopy (AFM) has a nanoscale resolution, which provides an effective tool for scientists to observe how atoms and molecules gather into crystals. In 2000, Yau and Vekilov (Yau and Vekilov, 2000) used atomic force microscopy to observe the structure of the quasi planar nuclei of apoferritin, and observed how molecules or clusters of molecules in solution were arranged in an ordered way. At the same time, the near critical nucleus of macromolecular protein is not spherical, but flat, such as boat.

Chunsheng et al (Chunsheng et al., 1994) analysed the nucleation process from the viewpoint of thermodynamics, and pointed out that the existence of additional pressure

can greatly affect the critical nucleation radius and critical nucleation free energy. Wenjun et al. (WenJun et al., 2000) explored the microscopic dynamics of nucleation mechanism. It is pointed out that the nucleation rate can have a great influence on the crystal size and its distribution. It is found that the internal factors affecting the crystal size are the formation energy of the aggregate and the lattice energy of the product. Based on the two-step nucleation theory, Zheng Pingyou et al (ZHENG Pingyou, 2006) analysed the nucleation and growth kinetics of the evaporative crystallisation process, and established the theoretical model of nucleation and growth process.

At the same time, the factors affecting the crystal size distribution, such as temperature, supersaturation, and particle size, are analysed, and a mathematical model with multiple parameters is established. Yang Liu et al. (YANG Liu 2008) developed a set of on-line measuring equipment for primary nucleation induction period based on conductivity method. The experimental nucleation induction period was fitted by classical nucleation theory model, and several factors in primary nucleation process were explored. It includes critical nucleation free energy, critical nucleation radius and interfacial tension of solid-liquid surface. (Song Meifeng 2004) the critical nucleation radius and nuclear barrier were determined by comparing the free energy of homogeneous nucleation and heterogeneous nucleation, and the formation process of nucleation was investigated. Huang Linjun et al. (Huang et al., 2014) summarised the classical nucleation theory from the aspects of thermodynamics and kinetics, and analysed its shortcomings and made corrections: The two step nucleation theory is introduced from several aspects of nucleation rate, computer simulation, theoretical basis and experimental research, and the relations and differences between the two theories are analysed.

2.3 Light Scattering Technology

light scattering technology has been widely used in chemical, biological and other

research areas, especially in the process of nucleation and growth of protein solutions. With the development of science and technology, light scattering technology has greatly improved in many aspects. It can be used not only in ground experiments, but also in space. Moreover, light scattering technology has many advantages, such as easy detection, no damage to samples, the detection process is fast (McPherson, 1997). Light scattering technique was first used to study protein crystallisation process in 1978.

Static light scattering (SLS) can measure the molecular weight of protein and get the interaction relationship between proteins. Dynamic light scattering (DLS) can measure the aggregation behaviour of protein molecules in the solution, the fluid dynamics radius and distribution of aggregates.

The application of light scattering in the nucleation of proteins is mainly manifested in the following aspects:

2.3.1 Control of nucleation and growth stages of crystals

In order to achieve this goal, it is common to use some methods to reduce the over - saturation of the solution, such as changing the solution's degree of saturation of the solution , such as changing the solution temperature(Rosenberger et al., 1993) , dilute the mother liquor under the nucleation condition(Saridakis et al., 1994) , etc . However, no matter what method is employed, a large amount of crystal nucleus can be produced in the solution before crystals can be observed under a microscope. Bulk crystallisation, liquid - liquid diffusion crystallisation, evaporation diffusion crystallisation, those method could hardly completely separate nucleation and growth(Mikol et al., 1989). In the initial stage of nucleation, the protein molecules in the solution are continuously aggregated into clusters, and the light scattering intensity of the solution can be observed obviously by using a dynamic light scattering instrument (DLS), so that the nucleation and growth can be distinguished according to the change of light scattering intensity. By optimising some experimental conditions, such as temperature of solution,

concentration of protein, concentration of precipitator and so on, the rate of oversaturation of solution can be reduced, which can be used to control the nucleation process of solution dynamically. Dynamic light scattering (DLSs) can be used to measure different forms of protein molecules, such as protein morphology before nucleation and after aggregation nucleation and protein crystal (Mikol et al., 1989).

2.3.2 Determination of translational diffusion coefficient, particle size and distribution of particles in solution

Dynamic light scattering can measure the translational diffusion coefficient of particles in solution (Baritaki et al., 2002) because the particles in the solution are in Brownian motion all the time, because of the different intensity of Brownian motion of particles of different sizes. The intensity of light scattering signal can be used to quantitatively analyse protein behaviour. Dynamic light scattering technique has been widely used in the observation of particle size change and its distribution in protein solution, it is also able to measure induction period of nucleation process(Malkin and McPherson, 1993)and acknowledge the interaction between protein molecules . In order to study the nucleation process of proteins, the changes of aggregates in supersaturated solutions with time can be explored.

Dynamic light scattering can be used to explore how molecules gather and nucleate in solution, and to determine the size and distribution of protein molecules and aggregates (Weetall and Gaigalas, 1993). Both nucleation and growth process are closely related to the behaviour of aggregates, and the monodispersity of the solution will greatly affect the quality of the crystals. The monodispersity of biopolymer solution (Phillips et al., 1997) can be determined by dynamic light scattering, which is helpful to further understand the nucleation and growth process and finally to produce good protein crystals.

2.4 Focused Beam Reflectance Measurement

The Focused Beam Reflectance Measurement (FBRM) is a valuable analytical technique widely employed in various industries, such as pharmaceuticals, chemical engineering, and food processing, for real-time monitoring and characterisation of particle size distributions and changes in dispersions and suspensions. Developed by Lasentec (now part of Mettler-Toledo), FBRM offers unique capabilities for understanding and optimising complex processes involving particles or droplets.The methodology of FBRM involves a systematic approach to real-time monitoring and characterisation of particle size distributions and changes in dispersions and suspensions. It begins with a focused laser probe that is directed into a sample containing particles or droplets of interest. As these particles traverse the path of the laser beam, they scatter light in various directions.

The key component in FBRM is the backscatter detection system. Positioned opposite to the laser source, a highly sensitive photodetector captures the intensity of light scattered (backscattered) by the particles. This captured backscatter data holds crucial information about the particle size and count within the sample.

Subsequently, advanced data analysis techniques are employed through FBRM software. This software analyses the fluctuations in backscatter intensity over time, effectively converting these fluctuations into valuable data. From this analysis, FBRM derives information regarding the number of particles, their sizes, and any changes occurring in their properties within the dispersion or suspension.

FBRM has found numerous applications in many fields. In pharmaceutical crystallisation processes, FBRM is crucial for real-time monitoring of particle size and shape, enabling precise control to ensure the production of high-quality crystals and

powders. In chemical Engineering, FBRM aids in optimising processes involving precipitation, agglomeration, and crystallisation. It helps prevent unwanted particle growth, agglomeration, and fouling. In Food Processing: The technology is used to monitor and control emulsions, ensuring product stability and uniformity (Heath et al., 2002).

2.5 Ultrasonic Spectroscopy Technique

Ultrasonic attenuation spectrum (UAS) is a promising online particle measurement method, similar in principle to light absorption and light scattering. This method measures the attenuation of ultrasonic waves passing through a sample and uses mathematical optimisation algorithms to deduce particle size distribution (PSD) information. As an advanced non-contact online measurement technique, UAS has significant potential for development. Compared to traditional methods like microscopy and light scattering, UAS offers advantages on: penetration capability, wide frequency range, non-contact, high resolution and accuracy, fast measurements, safety. However, there are limitations to using UAS for particle size measurements like sensitivity to air bubbles, measurement of material properties required and sensitive to temperature effects.

In recent decades, with the rapid development of electronic information technology and signal processing, significant progress has been made in ultrasonic signal processing and ultrasonic transduction technology. Researchers worldwide have increasingly focused on ultrasonic detection technology, particularly ultrasonic attenuation particle size measurement.

In 1953, Epstein introduced a theoretical model describing the interaction of ultrasonic waves with spherical particles. This model considered the viscous and elastic effects of

the liquid medium and the solid particles, as well as the influence of heat conduction. Building upon Epstein and Carhart's work, Allegra and Hawley extended the model to account for solid particle absorption and scattering effects, leading to the development of the Epstein-Carhart-Allegra-Hawley (ECAH) model. The ECAH model provided a theoretical foundation for ultrasonic attenuation particle size measurement.

Researchers like R.E. Challis from the University of Nottingham further refined and modified the ECAH model. Additionally, Harker and Temple introduced the Harker and Temple model, considering the dominant role of viscosity in dilute suspensions. In recent years, D.J. McClements has become an expert in ultrasonic attenuation theory and its application to particle size measurement in food emulsions. His contributions have significantly advanced the field.

These researchers' efforts have not only driven the rapid development of ultrasonic attenuation theory but have also provided technical support for the instrumentational production of this technology. For instance, Mougin in the UK accurately measured the relationship between sound attenuation, ultrasonic frequency, and crystal particle size distribution during the crystallisation process using Malvern's ultrasonic attenuation spectrometer. This enabled online monitoring of crystallisation processes. Germany's Sympatec GmbH produces the OPUS online particle size analyser, capable of accurately measuring micrometre-sized particle sizes in suspensions.

In summary, ultrasonic attenuation spectroscopy is a versatile and promising technique with various applications across industries, supported by continuous advancements in theory and technology.

2.6 Summary

In this Chapter, the theoretical basis of nucleation process is summarised, and two kinds of nucleation theories are introduced: The classical nucleation theory and the two-step nucleation theory. The classical nucleation theory describes the nucleation process in terms of thermodynamics and dynamics. Based on some hypotheses of the classical nucleation theory, its limitations are summarised. It is concluded that classical nucleation dynamics can be used to calculate the critical nucleation radius and nucleation rate, but it cannot obtain the path of the solute molecules to form a collective and the inner structure of the nucleation. The research progress of nucleation process at home and abroad is summarised. The study of nucleation theory and nucleation process plays a great role in the study of light scattering technology from the control of crystal nucleation and growth stage and the determination of translational diffusion coefficient of particles in solution. Various PSD measurement methods are also briefly summarised in this chapter.

CHAPTER 3. ULTRASONIC ATTENUATION FOR PARTICLE SIZING

3.1 Basic Principle

3.1.1 Basic concept of ultrasonic attenuation and sound attenuation mechanism

Sound waves are a transmitting form of object mechanical vibration, band above 20 kHz is defined as ultrasonic, while band below 20Hz is defined as infrasonic. There are three kinds of vibration forms of sound waves, transverse wave, longitudinal wave and surface wave, both of them exist in sounds. For ultrasonic, the main vibration form is longitudinal wave(Cheeke, 2012).

The reason for studying ultrasonic is because it has many applications. These occur in a very broad range of disciplines, covering chemistry, physics, engineering, biology, food industry, medicine, oceanography, seismology, and so on. Nearly all of these applications are based on two unique features of ultrasonic waves:
Ultrasonic waves travel slowly, about 100,000 times slower than electromagnetic waves. This provides a way to display information in time, create variable delay, and so on.
Ultrasonic waves can easily penetrate opaque materials, whereas many other types of radiation such as visible light cannot. Since ultrasonic wave sources are inexpensive, sensitive, and reliable, this provides a highly desirable way to probe and image the interior of the opaque objects. Ultrasonic also has features of well directional, easy to get and long travel distance in the liquid.

When ultrasound travels in the medium, the sound intensity will gradually decrease with the distance increase, this phenomenon is called sound attenuation. There are three types of sound attenuation: diffusion attenuation, scattering attenuation, and absorption

attenuation. The diffusion attenuation is related to the characteristics of the sound source, and the attenuation and absorption attenuation are related to the propagation medium of the acoustic wave. Therefore, in general, the diffusion loss is taken into account in the calculation of acoustic loss, and the scattering loss and the absorption loss are taken into account when considering the relationship between the acoustic wave and the medium. The previous studies found that the main reason of causing ultrasonic attenuation in the particle two-phase flow are absorption loss, energy loss, and scattering loss. The loss mechanism will be briefly introduced on below.

Absorption loss

Absorption loss is the absorption of sound waves by the medium itself, usually, when the concentration of the suspension is low or the particle size is small, the loss caused by this internal absorption mechanism is considered. This loss occurs due to the fact that the ultrasonic wave direct effect with the medium of two-phase flow and particles at the molecular level.

Energy loss

a. Viscous loss

The viscous loss is mainly due to the difference in density between the particles and the medium, and the density difference causes the particles relative motion in the continuous medium. This not fixed sliding motion is called the shear wave, which is the main reason for the loss of viscosity. For rigid particle particles with the diameter less than 3 μm, this viscosity loss mechanism is dominant.

b. Heat loss

As the temperature and pressure of the particle surface will produce thermal coupling effect, the wave will loss heat. In the compressed area of the wave, the pressure and temperature will rise at the same time, and when the molecules with higher temperature move to the lower temperature area, the pressure of compression is reduced, so the

amplitude of the wave is reduced. This loss mechanism usually plays a dominant role in small non-rigid particles or in various polymer colloids and emulsions.

c. Scatter loss

In essence, the scattering of sound is consistent with the scattering of light, except that the light is converted into other forms of energy during the scattering process and the sound flow is only changed in the direction so that the energy reaching the receiver is reduced, which the ultrasonic attenuation is caused by scattering. When the ultrasonic frequency is higher than 100MHz or the particle diameter is larger than 1μm, the scattering has a significant effect on the attenuation loss, and the scattering loss decreases rapidly with the decrease of particle size (Li, 2015).

When sound travel through a suspension of particles, the degree of attenuation depends on: the physical properties of the dispersed phase and dispersed medium, volume concentration of sample, particle size distribution (Falola, 2015).

3.1.2 Ultrasonic Attenuation Spectrometer (UAS)

The basic theory of ultrasonic attenuation method for measuring particle size distribution can be summarised as: based on a suitable theoretical model, the physical properties of the dispersed phase particles and the dispersed medium are known, describe the acoustic propagation process of a two-phase mixture of arbitrary predetermined particle size distribution and volume concentration, the theoretically predicted value of the sound attenuation as a function of frequency, i.e. the sound attenuation spectrum, and a model matrix of the relationship between the reactive particle system and the acoustic attenuation velocity spectrum will be obtained. At the meantime, the acoustic attenuation coefficient and the sound velocity are obtained by using ultrasonic attenuation measurement of the sample, and the optimal particle size distribution and particle phase concentration are obtained by data inversion combined with the model matrix. The data inversion here means that the theoretical model predicts

the relationship between a set of ultrasonic attenuation values and frequency and compares it with the actual measured values. The difference between the two is defined as the error function. By solving the function with the least squares method, minimum the value of the error function, the smaller the error, the more consistent the predicted particle size distribution with the true value.

A particle size distribution measurement system consists of three main components:
Signal generating and acquisition system or ultrasonic attenuation spectrometer: This is the electronic components used to measure the frequency dependent attenuation spectrum.
Ultrasonic attenuation model: This is the model that can be used to determine the attenuation spectrum from the physical properties of the sample.
Control software: is the software used to control the signal acquisition system and is equipped with some form of optimisation algorithm(s) to extract the particle size distribution from the measured attenuation spectrum.

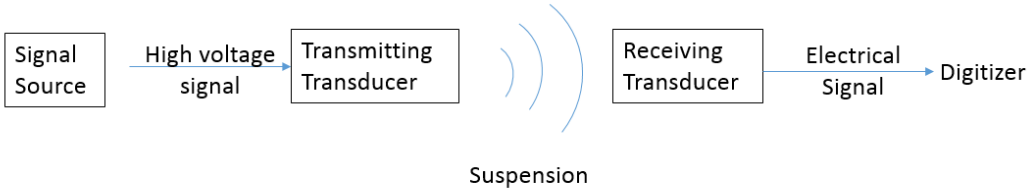

Figure 3.1 Ultrasonic attenuation spectrophotometer concept map

Figure 3.1 shows the basic setups of a UAS system in through transmission and pulse-echo modes respectively. It consists mainly of an excitation source that generates high voltage signal used to excite the transmitting transducer to emit the ultrasonic wave into the sample. The ultrasonic wave travel through the sample and is converted back to an electrical signal by the receiving transducer. The digitiser (or oscilloscope) is used to

sample the signal from the receiving transducer to produce digital signals that can be read by the computer.

The signal acquisition of the spectrometer can be operated in two modes:

1. Through-transmission mode: In this mode, two separated transducers are employed: one to generate the wave and the other to receive the wave. The signal source is sometimes connected to the transmitting transducer via a power-amplifier to boost the signal to noise ratio (SNR). Similarly, the receiving transducer can optionally be connected to a pre-amplifier to improve the SNR of the data acquisition (British Standards, 2006a). In through-transmission mode, it is important the transmitting and receiving transducers are properly aligned in order to avoid loss in the SNR of the data acquisition system (Challis et al., 2005).
2. Pulse-echo mode: In the pulse-echo data acquisition mode, the same transducer is used to both transmit and receive the ultrasonic signals. As in through transmission mode, power-amplifier and pre-amplifier can be employed to improve the SNR but, in this case, extra care is needed to prevent the transducer from being damaged by the excitation. Better SNR is obtained in this case when the face of the reflector is perfectly aligned to the face of the transducer and for very smooth reflector face. If the face of the reflector is not smooth enough or not parallel to the face of the transducer, the higher frequency data can become un-usable due to very low SNR (Challis et al., 2005).

3.1.3 Types of ultrasonic signals

There are many different signals that can be used to stimulate the ultrasound, depending on the particular application and the ultrasonic converter.

1) Continuous signal: continuous signal use for single-frequency or narrow-band

acoustic spectrometer .A radio frequency (RF) oscillator is used to generation and application of a single constant frequency signal to the transducer. The signal then passed through the sample and is reflected at both ends of the sample cell. If the signal is applied for a sufficiently long time, the acoustic signal will reach a constant value, the distance between the maximum values being a multiple of the wavelength of the wave.

2) Tone burst signal: Tone burst signal is used for wide-band sound acoustic spectrometer. Tone burst signal involves gating continuous signals of different frequencies to produce short bursts of signals applied to the ultrasonic transducers. The duration of each frequency burst must be shorter than the ultrasonic propagation time to prevent the overlap of two bursts at different frequencies.
3) Discrete frequency sweep is applied to windowed continuous waves at different frequencies, where each frequency is applied for a sufficient time to produce a constant value wave. Then the frequency gradually increases from low to high. It should be noticed that only the frequency step is not shown for the actual ultrasonic signal.
4) Broadband pulse: This involves the application of broadband video pulse to the transmitting transducer. Broadband pulse method is a wide bandwidth method, but with the pulse and broadband pulse method is different from the sensor only transmit a single signal. The frequency information in the pulse is extracted by using a frequency analysis method such as a fast Fourier transform (FFT) method. Compared with other wide bandwidth methods, broadband pulse acquisition time is shorter, and the signal to noise ratio (SNR) is lower.

In order to improve the signal to noise ratio (SNR), most measurement systems are associated with continuous measurement averages. The SNR improves by a factor of $\sqrt{N}$ for N coherent averages (Challis et al., 2005, Chen, 2007). The SNR limits the frequency bandwidth of the measurable attenuation spectrum. The noise level is usually

high at extreme frequencies close to zero frequency and twice the centre frequency of the sensor (Challis et al., 2005). Some commercial instruments such as the Malvern Ultrasizer optimise the SNR by adjusting the distance between the transmitting and receiving transducers: for highly attenuated systems, the distance decreases and the distance increases for less attenuation or dilution systems.

3.2 Models for Acoustic Attenuation Calculation

The models for calculation acoustic attenuation in a suspensions and emulsions can be generally classify into three categories.

3.2.1 ECAH model

In 1953, Epstein proposed a mathematical model in his paper. This model considering the elastic effects of solids and the viscous viscosity of the liquid, and also considering the effects of heat conduction (Epstein and Carhart, 1953).After this work, Allegra and Hawley developed the model to make it suitable for the suspension. This model is Epstein-Carhart-Allegra-Hawley model, also known as the ECAH model (Allegra and Hawley, 1972). The ECAH model has a comprehensive consideration of the mechanism loss, heat loss, scattering loss, viscosity loss and absorption loss. It is a mathematical model which is a milestone in this field of particle size distribution measurement by ultrasonic attenuation method.

The ECAH model assumes that the particles under examination are monodisperse, isotropic spherical particles, and it neglects interactions between particles. The wave equation for sound in the dispersed phase and continuous phase is derived based on the laws of conservation of momentum, mass, and energy, as well as the thermodynamic state equation. Solving this wave equation in spherical coordinates involves expanding

it into series using spherical Bessel functions and spherical Hankel functions. This expansion includes the undetermined scattering coefficients. Applying boundary conditions at the particle-medium interface typically results in a system of linear equations of sixth order. Solving this equation system allows one to obtain the scattering coefficients associated with the complex wave number. Here, the wave equation is provided:

$$\begin{aligned}(\nabla^2 + k_c^2)\phi_c &= 0\\ (\nabla^2 + k_T^2)\phi_T &= 0\\ (\nabla^2 + k_s^2)A &= 0\end{aligned} \tag{3.1}$$

where k_c is compressional wavenumber; k_T is thermal wavenumber; k_s is shear wavenumber. These complex wavenumbers k_c, k_T, and k_s can be determined using the following equations:

$$\begin{aligned}k_c &= \frac{w}{c} + i\alpha\\ k_T &= (1+i)\sqrt{\frac{w\rho C_p}{2\kappa}}\\ k_s &= \sqrt{\frac{w^2\rho}{\mu}}\end{aligned} \tag{3.2}$$

Where $i = (-1)^{1/2}$; C_p refers to the specific heat capacity at standard pressure; ρ refers to the density of the continuous phase medium. μ refers to the shear modulus of the particles.

The above equations are applicable to both the dispersed phase and the continuous phase. If the dispersed phase consists of viscous liquid particles, then μ can be replaced by $iw\eta$.

Under spherical symmetry conditions, solving equation (3.1) using Legendre

polynomials results in the following compressional wave function relationship for a suspension system:

In Suspension system:

$$\begin{aligned}\phi_0 &= \sum_{n=0}^{\infty} i^n\,(2n+1) j_n(k_c r) P_n(\cos\theta)\\ \phi_c &= \sum_{n=0}^{\infty} i^n\,(2n+1) A_n h_n(k_c r) P_n(\cos\theta)\\ \phi_T &= \sum_{n=0}^{\infty} i^n\,(2n+1) B_n h_n(k_T r) P_n(\cos\theta)\\ A &= \sum_{n=0}^{\infty} i^n\,(2n+1) C_n h_n(k_s r) P_n{}^1(\cos\theta)\end{aligned} \tag{3.3}$$

Inside the sphere:

$$\begin{aligned}\phi_c' &= \sum_{n=0}^{\infty} i^n\,(2n+1) A_n' j_n(k_c' r) P_n(\cos\theta)\\ \phi_T' &= \sum_{n=0}^{\infty} i^n\,(2n+1) B_n' j_n(k_T' r) P_n(\cos\theta)\\ A' &= \sum_{n=0}^{\infty} i^n\,(2n+1) C_n' j_n(k_s' r) P_n^1(\cos\theta)\end{aligned} \tag{3.4}$$

where

j_n is n-th order spherical Bessel function.

h_n is n-th order spherical Hankel function.

P_n is n-th order Legendre polynomial.

A and A' is non-zero matrices.

To solve the above equation, at the surface of the spherical particle, boundary conditions for the continuity of sound velocity, temperature, stress components, and heat flux are given. Under axisymmetric conditions:

$$\begin{gathered} v_r = v_r' \\ v_\theta = v_\theta' \\ T = T' \\ \tau \frac{\partial T}{\partial r} = \tau' \frac{\partial T'}{\partial r} \\ P_{rr} = P_{rr}' \\ P_{r\theta} = P_{r\theta}' \end{gathered} \tag{3.5}$$

Epstein pointed out in the literature that the total acoustic wave attenuation is determined by the coefficient An. Due to the coupled relationships between scattering coefficients, it is not possible to calculate an individually, and it can only be obtained by solving the above 6th-order linear system of equations. However, both the aforementioned boundary conditions and the process of solving the 6th-order linear system of equations are quite complex. The final expressions for the attenuation coefficient and complex wave number are:

$$\alpha_s = -\frac{3\phi}{2k_c^2 R^3} \sum_{n=0}^{\infty} (2n+1)\, A_n \tag{3.6}$$

where αs is the acoustic attenuation coefficient of the suspension.

Furthermore, by calculating the approximate values of wave numbers, the total acoustic attenuation and sound velocity can be obtained, which is also the case for most of the ultrasound instruments measurement results provided both domestically and internationally. The equation is directly given as follows:

$$k = k_c - \frac{3i\phi}{2k_c^2 R^3}\sum_{n=0}^{\infty}(2n+1) = \frac{w}{c} - i\alpha \tag{3.7}$$

Where k is the frequency related to the wave number (Hz).c is the speed of sound m/s. α is the total acoustic attenuation, in Np/m.

Allegra and Hawley pointed out that ECAH is based on the study of single particle scattering and is generally applicable to dilute solutions. There are still limitations in particle measurements for high-concentration solutions. Under high-concentration conditions, it is necessary to consider the interactions between particles and the phenomenon of multiple scattering of particles. To address this issue, many experts and scholars, such as Foldy, Waterman and Truell, Lloyd and Berry, have established theoretical models that consider multiple scattering effects based on practical measurement needs. This paper will not delve into this topic extensively.

ECAH model is the basic of most scattering models but is limited to dilute suspensions because the model was derived for an isolated particle with no particle-particle interaction or multiple scattering of the waves. There are also several formulations to improve the ECAH model such as the Waterman and Truell (1961) , Lloyd and Berry (1967) and Foldy (1945) formulations but these rarely improve the attenuation predictions at high solid volume fractions.

3.2.2 Core shell scattering model

The core-shell model of Hipp resolves the issue below. By deriving the scattering equations by assuming the particles are inserted in a shell of pure medium surrounded by an effective medium whose properties is a weighted average of the properties of the suspension (Hemar et al., 1997, Hipp et al., 2002).This model is more complex than the

ECAH model but it is found to give excellent prediction of the attenuation spectra over a wide range of particle size and volume concentrations. The scattering and core shell model however are computationally intensive and require careful implementations.

3.2.3 Coupled-phase model

While the scattering theories presented in the previous sub-sections take the microscopic approach to develop the ultrasonic theory, couple-phase theories are macroscopic approaches. In contrast to the scattering theories which are computationally and mathematically complex, the couple-phase models are usually very simple with minimal computational requirements. Therefore, the theories are very attractive especially for online measurement systems. While the scattering models are valid for all acoustic-wavelength, the couple-phase theories are only valid for low-acoustic radius for reasons to be explained later. The main advantage of most couple phase models is that they are self-consistent: the property of the mixture tends to that of the suspended material as the particle concentration increases (Challis et al., 2005, Evans and Attenborough, 1997).They therefore do not suffer from the “multiple scattering” problem encountered when using the scattering approaches. Another advantage is the fact that polydispersity is usually incorporated directly in the model.

The coupled phase models on the other hand are self-consistent but ignore the scattering effects on attenuation. They are therefore only valid for suspension with very small particles whose sizes are less than the wavelength of the sound wave. Harker and Temple and Dukhin and Goetz are two of the most popular coupled phase models and they are easier to implement compared to the scattering and core shell models and requires minimal computational power.

3.3 Attenuation Spectra Inversion to the PSD

In the last sections, the theoretical foundations of acoustic wave theory and attenuation theory were introduced. Regarding these theories, researchers are interested in using ultrasonic attenuation spectroscopy for non-contact measurement of particle size. Figure 3.2 illustrates the process of PSD measurement using ultrasonic attenuation spectroscopy. The fundamental idea is to input information such as material properties, temperature, concentration, particle size, and frequency range into the theoretical model. The theoretical model is then used to predict the ultrasonic attenuation spectrum, which is subsequently compared to the experimentally measured ultrasonic attenuation spectrum. This comparison ultimately yields the Particle Size Distribution (PSD) of the suspension or emulsion system.

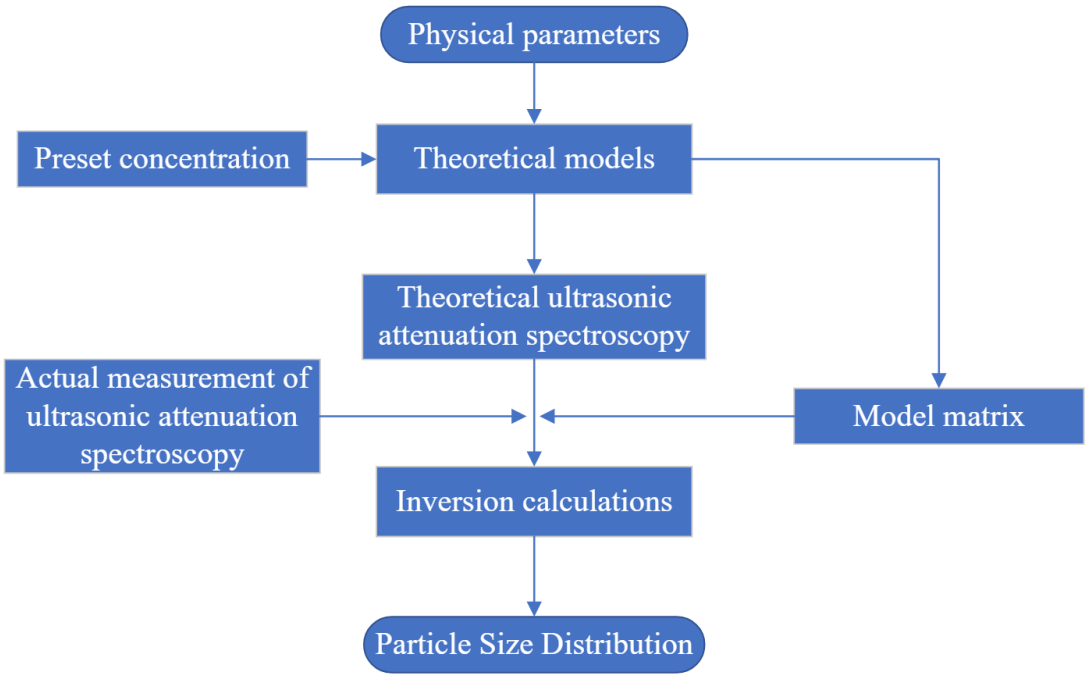

Figure 3.2 Ultrasonic Attenuation Spectrum Method Particle Measurement Process Schematic

In this case an error function is defined to quantify the difference between the predicted attenuation spectrum by the theoretical model and the measured attenuation spectrum. This error function can effectively evaluate the agreement between the actual particle size and the predicted particle size to some extent. Clearly, a smaller error indicates a higher degree of agreement and, consequently, a more accurate measurement. The error function is given by:

$$min_f = \sqrt{\frac{1}{N}\sum_{i=1}^{N}\left(\frac{\alpha_{measured}(i) - \alpha_{predicted}(i)}{\alpha_{measured}(i)}\right)^2} \tag{3.8}$$

Where $\alpha_{measured}$ is measured acoustic attenuation, Np·m^{-1}

$\alpha_{predicted}$ is theoretical model-predicted acoustic attenuation, Np·m^{-1}

The first type of Fredholm integral equation provides a functional relationship between particle size, measured acoustic attenuation, and model-predicted acoustic attenuation, and can be expressed as:

$$\alpha_{measured} = \int_{a_{min}}^{a_{max}} \hat{\alpha}(f,a) q_3(a) da \tag{3.9}$$

Where $\hat{\alpha}$ *is* the acoustic attenuation calculated by the model at different frequencies, Np·m^{-1}

a is the particle size in meters, m.

q_3 is the probability density function, m^{-1}。

Equation 3.9can be expressed in an equivalent summation form:

$$\alpha_{measured} = \int_{i=a_{min}}^{N=a_{max}} \hat{\alpha}(f, a_i) q_3(a_i) \Delta a_i \tag{3.10}$$

The transformation into matrix form is as follows:

$$\begin{bmatrix} \alpha(f_1) \\ \vdots \\ \alpha(f_n) \end{bmatrix}_{measured} = \begin{bmatrix} \hat{\alpha}(f_1, a_1) & \cdots & \hat{\alpha}(f_1, a_N) \\ \vdots & \ddots & \vdots \\ \hat{\alpha}(f_n, a_1) & \cdots & \hat{\alpha}(f_n, a_N) \end{bmatrix} \begin{bmatrix} q_3(a_i)\Delta a_1 \\ \vdots \\ q_3(a_N)\Delta a_N \end{bmatrix} \tag{3.11}$$

i.e.

$$b = Ax \tag{3.12}$$

In mathematical terms, the condition number of this matrix is relatively large, indicating that it belongs to the ill-posed matrix category. Special methods need to be sought for its solution. By observing the linear system of equations 3.12, it can be deduced that this matrix can be solved using the least squares method.

$$x = A^{-1}b \tag{3.13}$$

Or

$$\min_x \|Ax - b\| \tag{3.14}$$

Clearly, the particle size distribution is non-negative, with x≥0.

The drawback of this method is that the vector solution obtained is unstable, leading to oscillations and resulting in some error in the final measured attenuation values. Therefore, here we introduce a regularisation parameter γ_R to eliminate the impact of

noise on the matrix A during the solution process by using a filtering function. Combining it with the least squares method, we can derive the final particle size x as follows:

$$\min_{x}(\|(A^TA + \gamma_R HH^T)x - A^Tb\|)s.t.x \geq 0 \quad (3.15)$$

Where γ_R is regularisation parameter and $H=（A^TA）^{-1}A^T$.

Currently, the most widely applied optimisation criteria for the γ_R parameter are the Generalised Cross-Validation criteria (GCV) and the L-curve criteria.

GCV indicates that any omitted element in vector b should be predicted by the corresponding regularised solution. The regularisation parameter is independent of any orthogonal transformation in b. The optimal regularisation parameter can be obtained by minimising the following objective function:

$$\min_{\gamma} G = \frac{\left\|(A^TA + \gamma_R HH^T)x - A^Tb\right\|_2^2}{\left\{trace\left[1 - A(AA + \gamma_R HH^T)^{-1}A^T\right]\right\}^2} \quad （3.16）$$

The L-curve criterion refers to obtaining the optimal regularisation parameter by describing the double-logarithmic (log-log) residuals ‖Hx‖ and ‖Ax-b‖, resulting in a curve with an L-shaped appearance, hence the name. Typically, the optimal parameter γ_R is obtained at the saddle point of the curve.

Once the corresponding optimal regularisation parameter γ_R is obtained through the GCV criterion and the L-curve criterion, you can substitute it into Equation 3.15 to obtain the particle size distribution.

3.4 Summary

This chapter provides a systematic analysis of the fundamental issues and basic theory of the Ultrasonic Attenuation Spectroscopy (UAS) technique for particle size measurement.

Firstly, it begins by discussing the various aspects of ultrasound, including its types, propagation characteristics, speed of sound, and frequency, all of which are relevant factors for ultrasonic attenuation spectroscopy. This section enhances the understanding of ultrasound and concludes that it's possible to calculate particle size by measuring the ultrasound attenuation that occurs during its propagation through a medium.

Secondly, it describes the propagation and attenuation of ultrasound in pure media and dispersive systems, outlining the different attenuation mechanisms in various media. These mechanisms primarily include absorption loss, scattering loss, thermal loss, and viscous loss.

Next, it introduces several theoretical models that describe the propagation of ultrasound in two-phase systems, considering the various attenuation mechanisms. Among these models, the ECAH (Epstein-Carhart-Allerhand-Hawley) model stands out as the most classical theoretical model for describing sound scattering. It comprehensively takes into account the influence of all four types of losses, laying the foundation for the theoretical study of ultrasonic attenuation spectroscopy. However, it's noted that this model neglects the effects of particle interactions and complex scattering phenomena, making it suitable primarily for measuring particle sizes in low-concentration suspensions and emulsions.

Finally, the chapter provides a detailed explanation of the inversion calculation process of the ultrasonic attenuation spectrum using optimal regularisation algorithms.

CHAPTER 4. MATHEMATICAL OPTIMISATION ALGORITHM

Mathematical optimisation algorithms are powerful tools for solving real-world problems, helping us find the maximum or minimum of an objective function under given constraints. These algorithms are widely used in economics, engineering, physics, and business management, crucial for enhancing efficiency, reducing costs, and optimising resource allocation. The diversity of optimisation algorithms reflects their ability to tackle different types of problems. Each algorithm has specific applications and advantages, with the choice of algorithm often depending on the problem's characteristics and solution requirements. This chapter will introduce Genetic Algorithm, Parallel traversal algorithm, and Particle Swarm Optimisation.

4.1 Genetic Algorithm

Genetic Algorithm is a random search calculation method based on the evolution of the survival of the fittest in the natural world. The genetic algorithm starts from a population that may contain the potential solution set of the problems. After the first generation of the population, according to the principle of survival of the fittest, The evolution of generations produces a solution that is closer to the true value (Whitley, 1994).

The algorithm steps of the genetic algorithm are as follows:

1. Generating a random initial population, which include a certain number of individuals.
2. The strategy of roulette is used to determine the fitness of the individual. Since roulette is a random event, the result calculated by the genetic algorithm is a

random approximate solution. The results of multiple calculations are different, but they are all approximation of the true value. whether the optimisation criterion is met depended on individual fitness. If it is met, an optimal solution is output, thereby ending the calculation. If not, the next calculation is performed.

3. Selecting the regenerative individual according to the degree of fitness, individuals with low fitness may be eliminated.
4. Generate new individuals based on certain crossover methods and crossover probabilities.
5. Generate new individuals based on certain mutation methods and mutational probabilities.
6. The new generation of new individuals consisting of the fourth and fifth steps is returned to the second step for further calculation until the individual fitness meets the optimisation criteria as the output optimal solution.

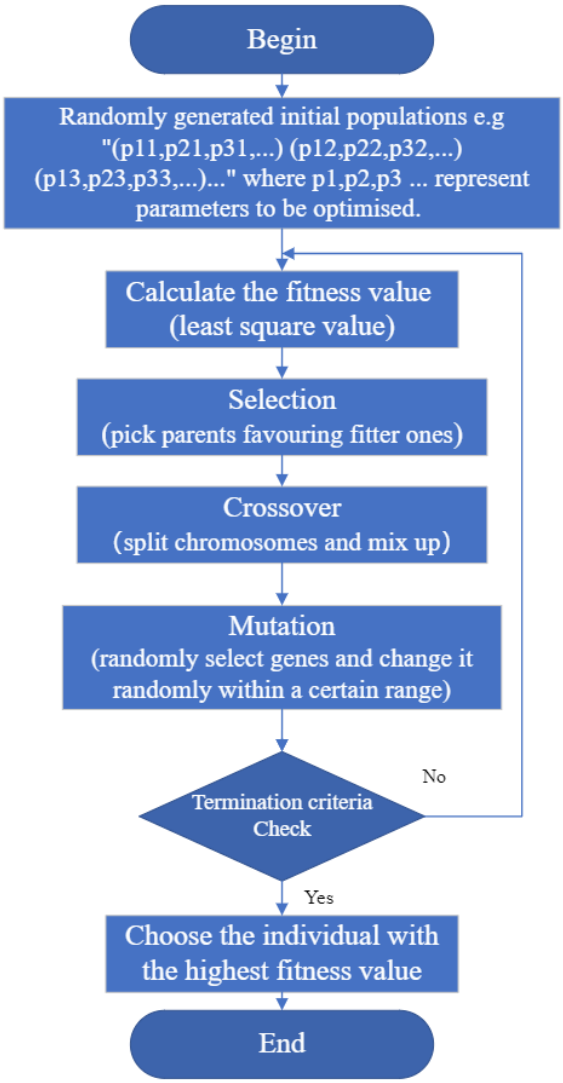

Figure 4.1 Genetic Algorithm Flow Chart

4.2 Parallel Traversal Algorithm

The genetic algorithm is more efficient, but the calculated results are random. The calculation results obtained by inputting the same value may be different when calculated multiple times. For the exhaustive method like parallel traversal, the input data will be calculated one by one, which will inevitably lead to lower efficiency. The final output value is the best result choice from all the calculation results. The randomness will be lower, and accuracy will be higher than genetic algorithms. When

the optimisation problem requires fewer data to be calculated, the parallel traversal method is selected because it saves time, and the calculated result is the closest to the true value. When the optimisation problem involves more data, the genetic algorithms should be selected for more efficiency.

4.3 Particle Swarm Optimisation, PSO

The particle swarm optimisation was invented by Eberhart and Kennedy (Kennedy and Eberhart, 1995). It is a stochastic search algorithm based on group cooperation, developed by simulating the foraging behaviour of bird flocks.

It should be noted that “particle” here means a “candidate solution”, i.e., a set of estimates for the parameters being optimised, thus equivalent to a chromosome in GA. Swarm is a collection of such particles, equivalent to population in GA.

Similar to genetic algorithms, particle swarm optimisation is an iterative optimisation algorithm. It starts by generating a set of random solutions and iteratively searches for the optimal solution. However, unlike genetic algorithms, particle swarm optimisation does not involve crossover and mutation operations. Instead, it utilises particles searching in the solution space to find the best particle.

Particle swarm optimisation can be likened to the foraging behaviour of a flock of birds searching for food in an area where only one food source exists. Each bird does not know the location of the food, but they are aware of the distance between themselves and the food. So, how do they determine the best way to search for the food? The simplest and most effective method is to search in the vicinity of the bird that is currently closest to the food.

By explaining the phenomenon of flock predation, particle swarm optimisation becomes easier to understand. In the algorithm, birds represent particles, and the food represents the optimal solution that the algorithm aims to find. The algorithm starts by initializing a group of random particles, which are the random solutions of the algorithm. Each particle has a fitness value determined by the function being optimised, and it also has a velocity that determines the distance and direction of its search.

Then, all particles search in a solution space, which is the area where the food is located. During the search process, each particle finds two optimal values: its current best position (pbest), which is the best position among all the positions it has searched, and the overall best position (gbest) found by the entire particle swarm. The next movement of each particle is determined by comparing these two values.

The steps of the Particle Swarm Optimisation algorithm are as follows:

1. Randomly initialize the velocity and position of each particle in the population.
2. Evaluate the fitness of each particle, store the fitness value and position of each particle in their respective pbest (personal best), and then store the fitness value and position of the particle with the best fitness in gbest (global best).
3. Update the velocity and position of each particle according to the following equation:

$$v_{i,j}(t+1) = \omega v_{i,j} + c_1 r_1 \left[p_{i,j} - x_{i,j}(t)\right] + c_2 r_2 \left[p_{g,j} - x_{i,j}(t)\right] \quad (4.1)$$

$$x_{i,j}(t+1) = x_{i,j}(t) + v_{i,j}(t+1), j = 1,2,\dots,d \quad (4.2)$$

Where ω is Inertia weight.

$c_1 c_2$ is positive learning factor.

$r_1 r_2$ is Random number uniformly distributed between 0 and 1.

4. Repeat steps 2 and 3 until a stop condition is met (e.g., reaching the maximum number of iterations or finding a satisfactory solution).

The core idea of this algorithm is to continuously update the velocity and position of particles through cooperation and information exchange among particles, gradually approaching the optimal solution. The pbest represents the best position found by each particle individually, while the gbest represents the best position found by the entire particle swarm. As the iterations progress, the velocity and position of particles are adjusted, ultimately converging to the global optimal solution or a close approximation.

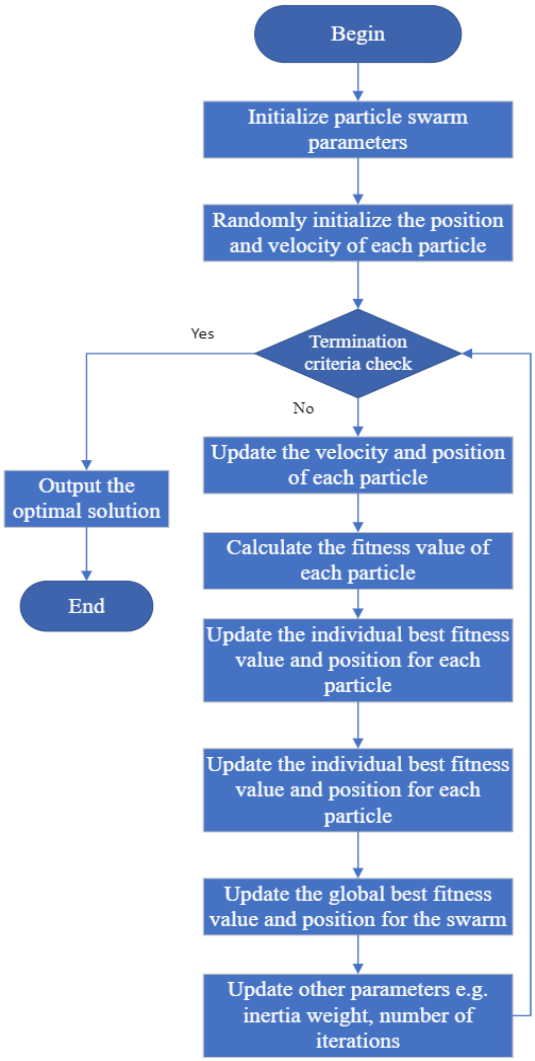

Figure 4.2 Particle Swarm Optimisation Flow Chart

It is worth noting that the effectiveness of the particle swarm optimisation algorithm is influenced by parameter settings, including population size, learning factors, inertia weight, etc. Choosing appropriate parameter values has an impact on the convergence and search ability of the algorithm.

4.4 Summary

Overall, there is no single algorithm that always has the shortest computation time in all scenarios. The choice and performance of an algorithm largely depend on the characteristics of the problem, the quality of the algorithm's implementation, and the available computing resources.

When the parameters required for optimising a problem are few, parallel traversal methods are more appropriate because the computations are not very time-consuming, and the results obtained will be the closest to the true values and the most accurate. However, when the data involved in the optimisation problem is extensive, advanced optimisation algorithms such as genetic algorithms or particle swarm optimisation algorithms are preferable. Genetic algorithms generally have better global search capabilities, but this also means that more iterations may be needed to find the optimal solution, thereby increasing computation time. Particle swarm optimisation algorithms may converge quickly in some cases, but if they fall into a local optimum, more iterations may be needed to escape the local optimum. Improving computational efficiency plays a crucial role in practical applications.

CHAPTER 5. RESULT

5.1 Introduction

A C++ based program was developed for physical parameter optimisation and PSD calculation optimisation completed. This program can utilise the Parallel traversal algorithm, Genetic algorithm, and Particle swarm optimisation algorithm method to optimise physical property parameters. It also has the capability to optimise PSD (Particle Size Distribution) results using the Mono, Uniform, Normal, Log-normal, and Weibull models individually, as well as the option to simultaneously optimise both of them.

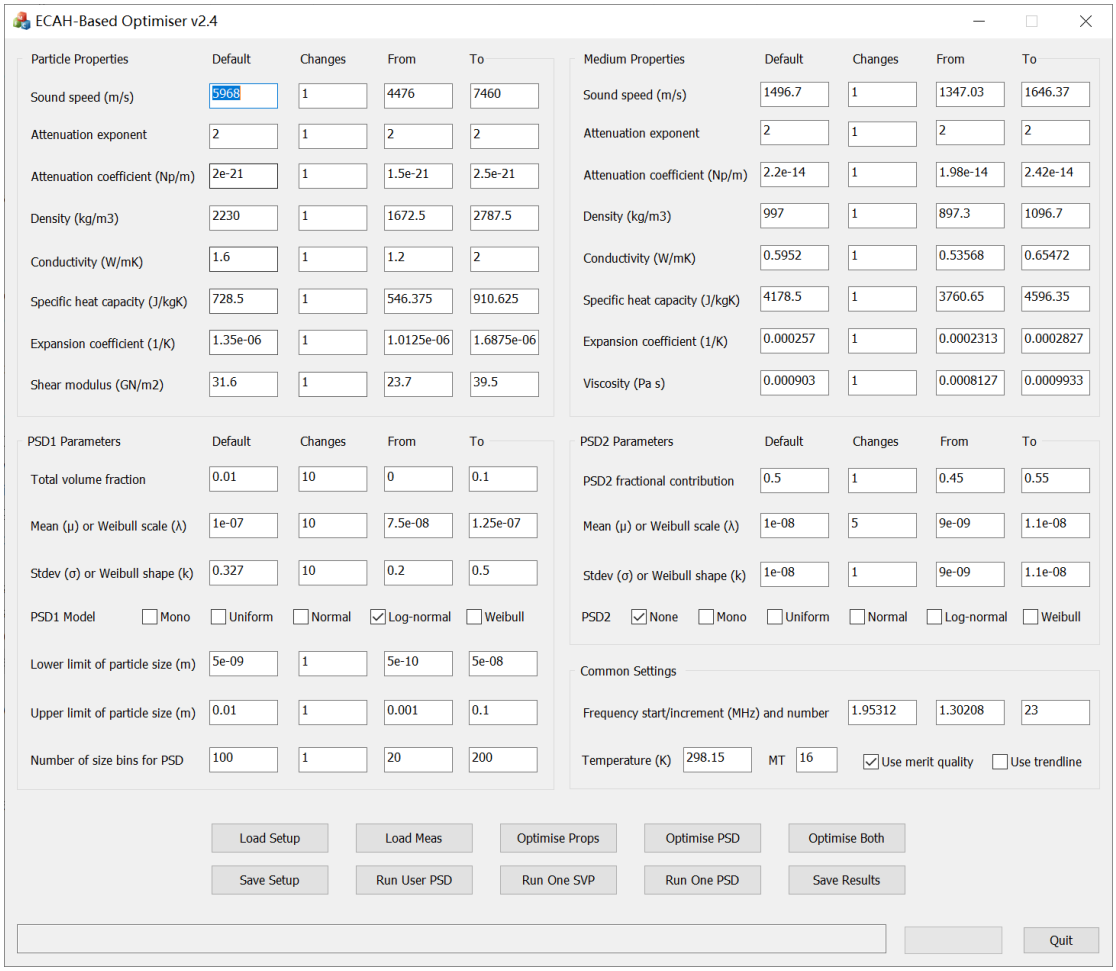

Figure 5.1 Interface of ECAH-Based Optimiser

Optimisation testing used the ultrasonic particle size analyser NanoSonic to obtain measurements of ultrasonic attenuation and particle size distribution. A SiO_2-H_2O suspension system with an average particle size of 100nm and a volume fraction of 1% at a temperature of 298.15K was used. The default physical parameters for this system are as follows:

Table 5.1 Physical Parameters SiO_2 and H_2O

Parameters	Water	SiO2
Sound Speed [m/s]	1496.7	5968
Shear Modulus [N/m^2]	N/A	3.16×1010
Attenuation Coefficient [Np/m]	2.2×10-14	2×10-21
Mass Density [kg/m^3]	997	2230
Viscosity [Pa•s]	9.03×10-4	N/A
Thermal Conductivity [W/mK]	0.5952	1.6
Specific Heat Capacity [J/kgK]	4178.5	728.5
Thermal Expansion Coeff [1/K]	2.57×10-4	1.35×10-6
Attenuation Exponent	2	2

5.2 Experimental Procedure

The instrument was calibrated using deionised water. Samples were prepared under controlled temperature at 298.15K. Deionised water was used as the continuous phase, and the suspension was ultrasonically dispersed for 15 minutes. The dispersed samples were transferred into a jacketed beaker and stirred magnetically at a moderate speed. The attenuation spectrum of the samples was displayed on the computer interface, with data collected every 30 seconds. Multiple datasets were obtained and analysed, selecting the dataset with the best fit for the attenuation spectrum. The particle size

distribution results obtained from multiple measurements were fitted to determine the average particle size and particle size distribution graph.

5.3 Sensitivity Check

Before conducting the primary optimisation of parameters and PSD, it is essential to perform sensitivity analysis on the parameters. This serves as a crucial preparatory step before attempting to adjust the parameter model. If the parameter significantly influencing the target result among the adjustable ones is identified, prioritising it for primary adjustments can enhance efficiency. Additionally, sensitivity analysis helps determine the approximate range of parameter variations, thereby preventing the tests beyond the limit of practical physical significance during the optimisation process.

Until now, there has been a lack of research tracking the sensitivity of changes in these specific physical parameters to attenuation results. Due to the intricate derivation process of ECAH, predicting sensitivity directly from formulas becomes challenging. Employing this testing approach not only accelerates the procedure but also enables the identification of potential thresholds. By combining theoretical formulas, precise threshold values can be calculated. Also, this is aimed at assessing the congruence of our program with the results obtained from ultrasound measuring instruments and calculations conducted using the ECAH optimiser. In the sensitivity analysis, variations of each parameter to observe the extent of changes in the attenuation results and assess whether the changes linearity. For results that non-linearity, an additional set of tests was conducted. Simultaneously, this testing process able to identify the range of parameter changes.

Table 5.2 Sensitivity (percentage change) of attenuation to Parameter at Frequency at 11.7188 MHz

Percentage Change	**110%**	**150%**	**200%**	**500%**	Comments
Particle					
Sound Speed	0.000894%	0.001182%	0.002460%	0.002811%	No significant change
Attenuation Coeff	0.000064%	0.000064%	0.000064%	0.000064%	No significant change
Density	32.62%	126.11%	467.84%	2270.09%	Linear change
Thermal Conductivity	-0.009871%	-0.026707%	-0.055262%	-0.089378%	No significant change
Specific Heat Capacity	0.10%	0.44%	1.14%	4.20%	Linear change
Thermal Expansion Coeff	-0.001533%	-0.006069%	-0.015173%	-0.059383%	No significant change
Shear Modulus	-0.000351%	-0.002971%	-90.349095%	-90.349095%	Nonlinear change
Medium					
Sound Speed	-8.12%	-23.47%	-30.93%	-69.65%	Linear change
Attenuation Coeff	0.96%	3.81%	9.62%	38.49%	Linear change
Mass Density	-22.88%	-62.90%	-88.84%	-42.94%	approximately Linear change
Thermal Conductivity	-0.014950%	-0.048881%	-0.108257%	-0.232836%	No significant change
Specific Heat Capacity	-0.109918%	-0.229127%	-0.444814%	-0.444814%	No significant change
Thermal Expansion Coeff	0.12%	0.60%	1.75%	14.03%	Linear change
Viscosity	-4.01%	-13.69%	-28.86%	-58.48%	Linear change

The Table 5.2 shows the result of sensitivity test of 14 parameters, Overall, variations in the parameters of the dispersed medium have a significant influence on ultrasound attenuation, while the influence of the dispersed phase is relatively minor.

The analysis of the testing outcomes is to be conducted in combination with the physical significance of the materials and the deductive process of the ECAH.

Ultrasonic travel in the dispersed phase exhibited significantly shorter duration compared to the dispersion refinement phase. Consequently, the thermodynamic and acoustic physical parameters of particles imparted a relatively minor influence on attenuation, though not entirely negligible.

The particle sound speed, particle attenuation coefficient, particle thermal conductivity and thermal expansion coefficient shows no significant change. The Attenuation Coefficient exhibits minor variations in attenuation values at 200-fold, yet these changes are not adequately manifested in the Table 5.2. The effect of sound speed within the dispersed phase on the result is relatively insignificant, whereas its influence within the medium is substantial and merits careful consideration. The reason why these parameters have little influence on the result is, firstly, because the coefficient of this parameter in the calculation process is small, and secondly, some of the parameters themselves are relatively small, and their changes will not have a large impact on the calculated result. These parameters will have a large range of changes in the subsequent optimisation process.

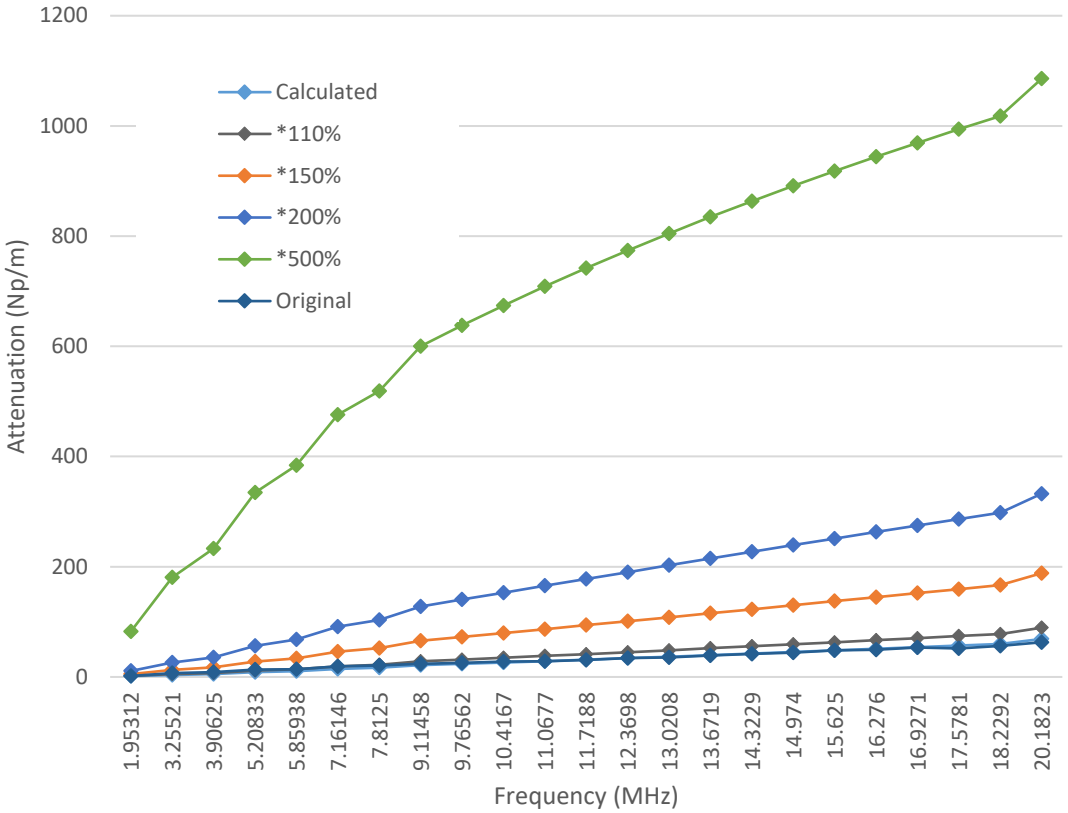

Figure 5.2 Attenuation of particle density sensitivity check

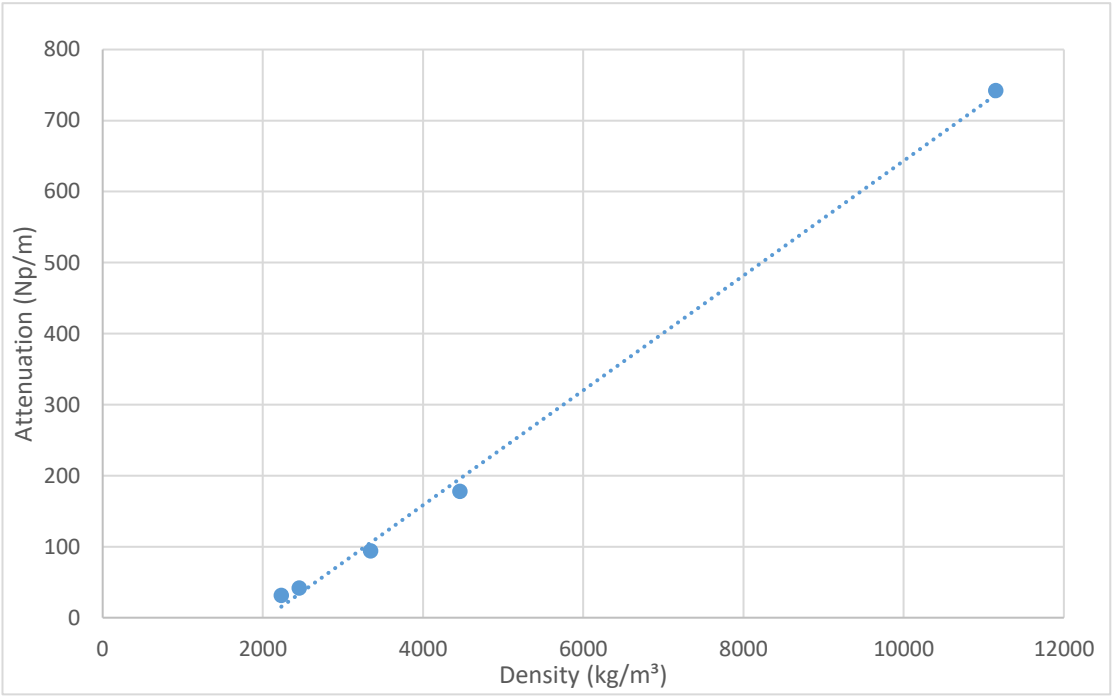

Figure 5.3 Attenuation of particle density at Frequency 11.7188 MHz in density sensitivity check

Particle density, particle specific heat capacity, medium attenuation coefficient, and medium viscosity shows approximately positive correlation linear change, and medium sound speed, medium density, medium thermal conductivity shows approximately negative correlation linear change. For example, Figure 5.2 illustrates the trend of attenuation values at various medium density, while Figure 5.3 demonstrates an increase in attenuation values with the growth of medium density at the specific frequency of 11.7188MHz. In order to render the results of parameter optimisation more practically meaningful and to reduce computational overhead, the subsequent process will entail a reduction in the range of change for these parameters.

Only the particle shear modulus sensitivity exhibits a nonlinear change, which is to be expected because shear modulus typically shows linear behaviour within the certain range, it can exhibit non-linear changes outside of this range or under varying conditions such as temperature and frequency. To ascertain the nonlinear range of shear modulus change, a set of diminished alterations is applied. According to Table 5.3.and Figure 5.4, when it exceeds the threshold of about 62 N/m^2, the Attenuation change results are no longer significantly affected by shear modulus change. The reason for this situation can be deduced from the derivation of the ECAH model. Therefore, in the subsequent optimisation computation, the upper limit of the shear modulus is constrained to 65 N/m^2.

Table 5.3 Sensitivity of attenuation to particle shear modulus at frequency 11.7188 MHz

Parameter Percentage Change factor	Attenuation change rate
20.0%	0.001416%
50.0%	0.000995%
66.6%	0.000765%
90.1%	0.000319%
110%	-0.000351%
150%	-0.002971%
200%	-90.349095%
500%	-90.349095%

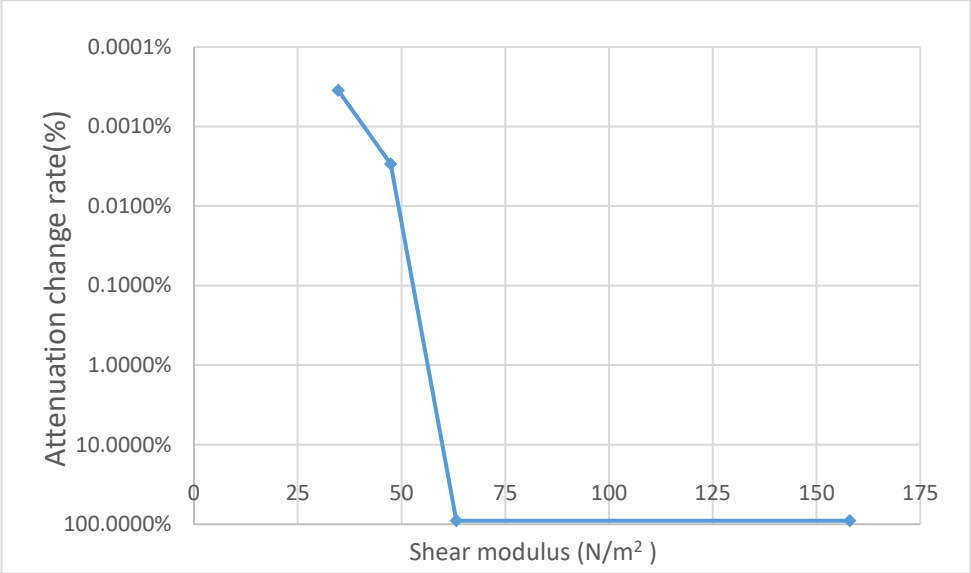

Figure 5.4 Attenuation change rate of particle shear modulus at frequency 11.7188 MHz

This testing iteration solely focuses on sensitivity assessment. To swiftly verify the correlation between parameter changes and ultrasonic attenuation, the most of parameters are tested with increased values only. The reduction of parameters will be assumed to follow the observed patterns from the testing for the decrease portion of parameters.

In summary, the variations in parameters such as particle sound speed, particle attenuation coefficient, particle thermal conductivity and thermal expansion coefficient exhibit minimal influence on the outcomes, thus warranting an expansion of their respective intervals during the parameter optimisation process. Conversely, the fluctuations in particle density, particle specific heat capacity, medium attenuation coefficient, and medium viscosity parameters yield substantial effects on the results, necessitating a reduction in their range of variations based on practical considerations. Furthermore, in the case of the Shear Modulus, it is advisable to constrain its maximum value to be below 65 N/m^2.

5.4 Parameter Optimisation

This chapter will focus on the optimisation of physical parameters. The testing includes single-parameter optimisation and simultaneous optimisation of multiple parameters. According to the results of the sensitivity testing of all parameters conducted in the last chapter. Each parameter was assigned specific ranges of variation, the Figure 5.5 and Table 5.4 elucidate a set of results where 7 parameters were optimised simultaneously. The parameters for the three algorithms are as follows:

- GA5: Genetic Algorithm with 5 changes per parameter, 2 number of elites to keep, 100 number of generations, 0.9 cross-over probability, 0.2 mutation probability, 0.1 diversity probability.
- PS5: Particle swarm optimisation method with 5 changes per parameter, 0.8 inertia weight constant, 0.1 cognitive coefficient, 0.1social coefficient.
- PT5: Parallel traversal algorithm with 5 changes per parameter.

From the attenuation Figure 5.5, it can be observed that all optimisation results fall between the original values and the theoretical calculated values, demonstrating the effectiveness of this approach.

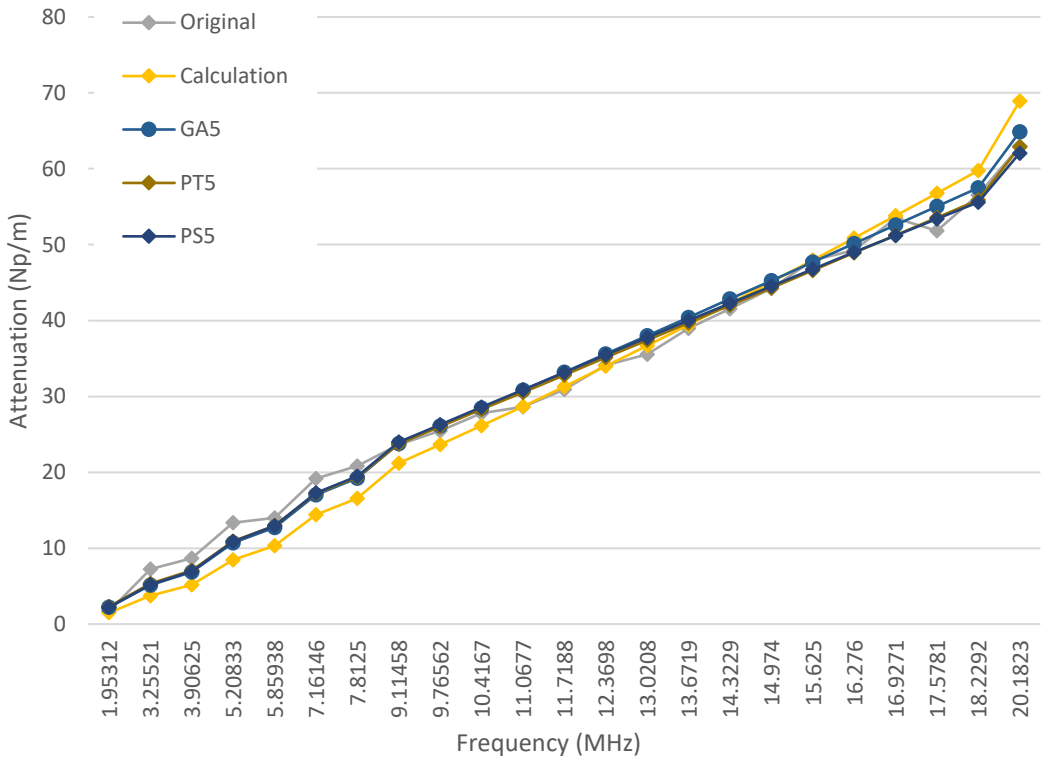

Figure 5.5 Attenuation of parameters optimisation

Table 5.4 Parameter optimisation result

Parameters	Original	GA5	PS5	PT5
Medium Attenuation Coeff	2.2E-14	1.98E-14	1.98E-14	2.20E-14
Medium Mass Density	997	1096.7	1096.7	963.767
Medium Thermal Expansion Coeff	0.000257	0.000707	0.0004	0.000554
Medium Viscosity	0.000903	0.0005	0.0005	0.000331
Particle Mass Density	2230	2230	2324.76	2044.17
Particle Specific Heat Capacity	728.5	2138.52	2755.8	655.65
Particle Shear Modulus	31.6	23.3789	12.1923	34.76

The optimisation of parameters follows the pattern of sensitivity testing. Insensitive parameters undergo substantial variations during optimisation and, therefore, require a wide range of variation to prevent reaching constraints during the optimisation process.

Conversely, highly sensitive parameters undergo minor changes during optimisation and, thus, are assigned a narrower range of variation, yielding more refined optimisation outcomes.

Single-parameter optimisation has been demonstrated to be feasible at the mathematical algorithm level in testing, but its optimisation results often exceed the physically reasonable values for that parameter. Since the ECAH algorithm is influenced by multiple parameters, significant changes need to be made to the optimised parameter during the single-parameter optimisation process to achieve the predicted results. For those insensitive parameters, such as particle sound speed, particle attenuation coefficient, particle thermal conductivity, and thermal expansion coefficient, their individual mathematical optimisation results often surpass the predetermined lower or upper limits, rendering the optimisation meaningless. In terms of runtime for single-parameter optimisation, PT is faster than PS and PS is faster than GA. For example, to optimise particle density, PT took 7.12 seconds, PS 42.72 seconds and GA 45.48 seconds.

Simultaneous optimisation of multiple physical parameters often yields better results, but it requires more powerful computational resources and longer computation times. In order to obtain more test results for comparison, this test only selected 7 sensitive physical parameters for simultaneous optimisation.

5.5 Particle Size Distribution Optimisation

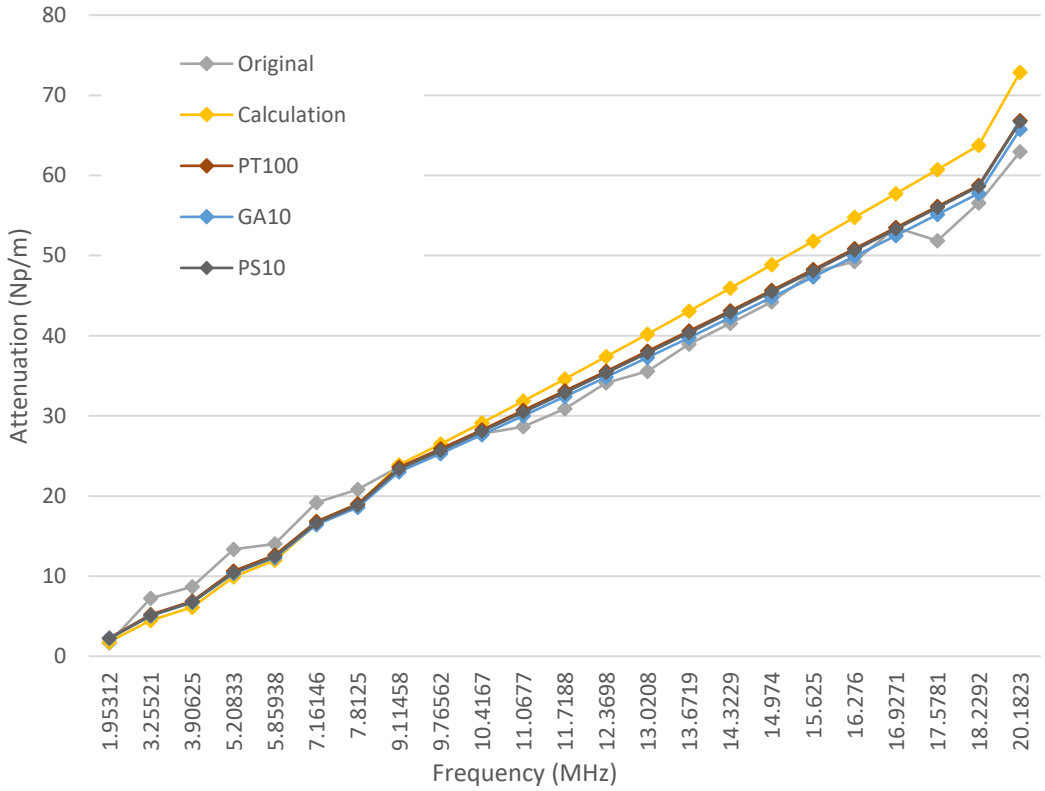

Figure 5.6 Attenuation of PSD optimisation

Figure 5.6 and Figure 5.7 illustrate the results of particle size distribution optimisation. the parameters for the three algorithms are as follows:

- GA10: Genetic Algorithm with 10 changes per parameter, 2 number of elites to keep, 100 number of generations, 0.9 cross-over probability, 0.2 mutation probability, 0.1 diversity probability.
- PS10: Particle swarm optimisation method with 10 changes per parameter, 0.8 inertia weight constant, 0.1 cognitive coefficient, 0.1 social coefficient,
- PT100: Parallel traversal algorithm with 100 changes per parameter.

Using the log-normal model. The range of particle size is set to 1e-10m ~ 5e-7m.

Number of size bin for PSD is set to 100. From attenuation Figure 5.5, it can be observed that all optimisation results fall within the range between original values and theoretical calculated values. This indicates the reliability of the physical parameter results obtained from all three optimisation algorithms. Runtime statistics are PT100 61.81 seconds (PT10 would be 0.65 seconds), GA10 58.23 seconds and PS10 60.22 seconds.

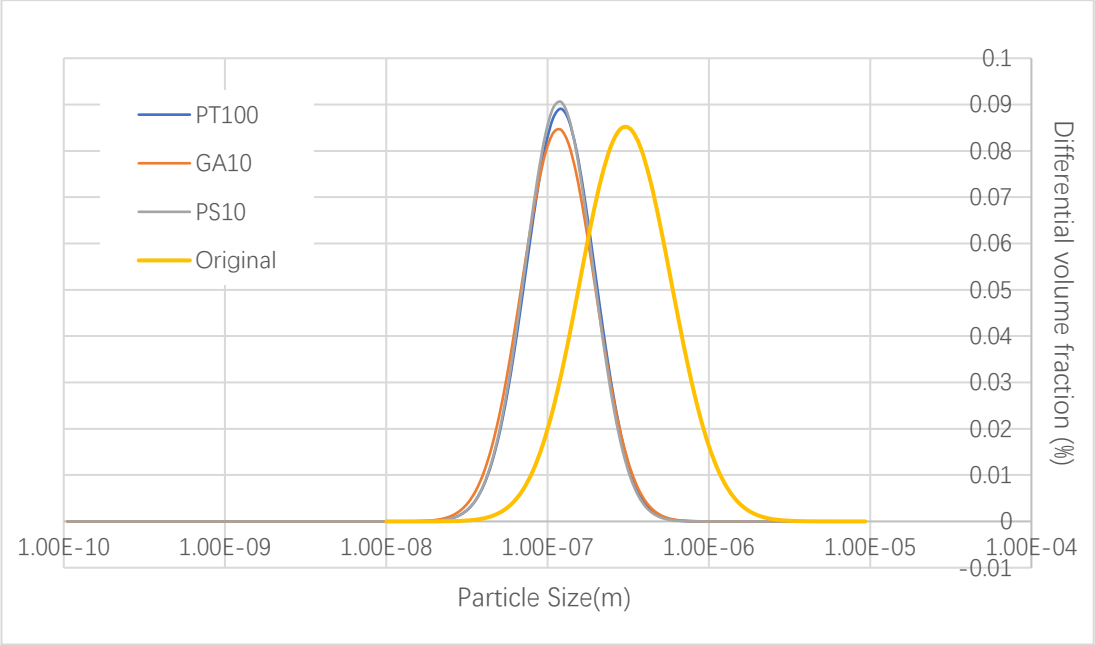

Figure 5.7 Distribution of PSD optimisation

Table 5.5 PSD optimisation result

	Original	PT100	GA10	PS10
PSD1_MeanScale(μ)	-15.701	-15.9184	-15.9495	-15.9377
PSD1_StdevShape(σ)	0.654	0.502041	0.527614	0.492949
PSD1_meansize(m)	1.52E-07	1.22E-07	1.18E-07	1.20E-07

In Table 5.5 its common for log-normal to use meanscale, and meanscale=ln(meansize), Meansize is used to represent the true value of the average particle size.

Due to the use of 100nm standard particles in this test, in the optimisation results, the closer the mean size is to 1e-7m and the smaller the standard deviation, the better the

optimisation performance. From Figure 5.7 and Table 5.5, it can be seen that the results obtained by the three optimisation algorithms meet the expectations. The results using the Mono, Uniform, Normal, Log-normal, and Weibull models are similar to the log-normal distribution.

5.6 Combined Parameter and Particle Size Distribution Optimisation

Combined optimisation is the process of optimise parameters and particle size distribution both. The combined optimisation results are more accurate but usually require a larger computational effort and longer processing time.

Table 5.6 Combined parameter and PSD optimisation result

Parameters	Default	PS5
Medium Sound Speed [m/s]	1496.7	1501.42
Medium Attenuation Coeff [Np/m]	2.20E-14	1.64E-18
Medium Mass Density [kg/m3]	997	984.932
Medium Viscosity [Pa.s]	0.000903	0.00079091
Particle Mass Density [kg/m3]	2230	2174.63
PSD1 Mean Scale	-15.701	-15.5526
PSD1 Stdev Shape	0.654	0.201

The Table 5.6 show the result of combined optimisation. 7 parameter is optimised in this case, using Particle Swarm algorithm with 5 changes per parameter, 0.8 inertia weight constant, 0.1 cognitive coefficient, 0.1social coefficient, PSD optimisation using the log-normal model. The range of particle size is set to 1e-9 m ~ 5e-7 m. Number of size bin for PSD is set to 100.

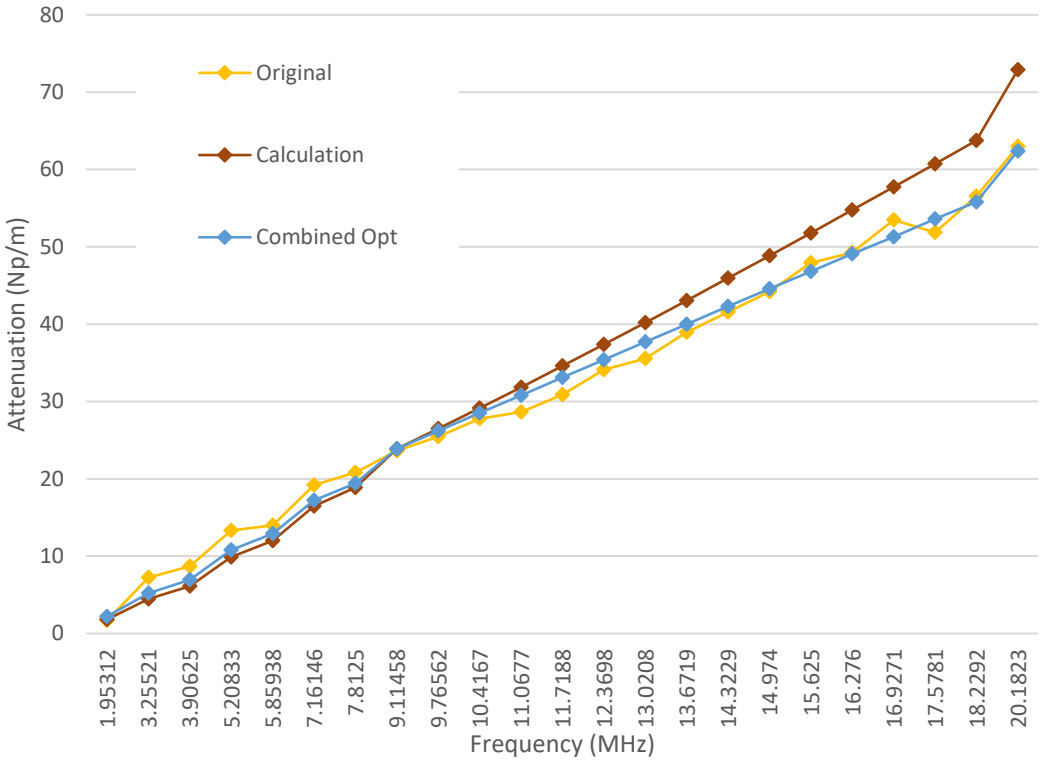

Figure 5.8 Attenuation of Combined parameter and PSD optimisation

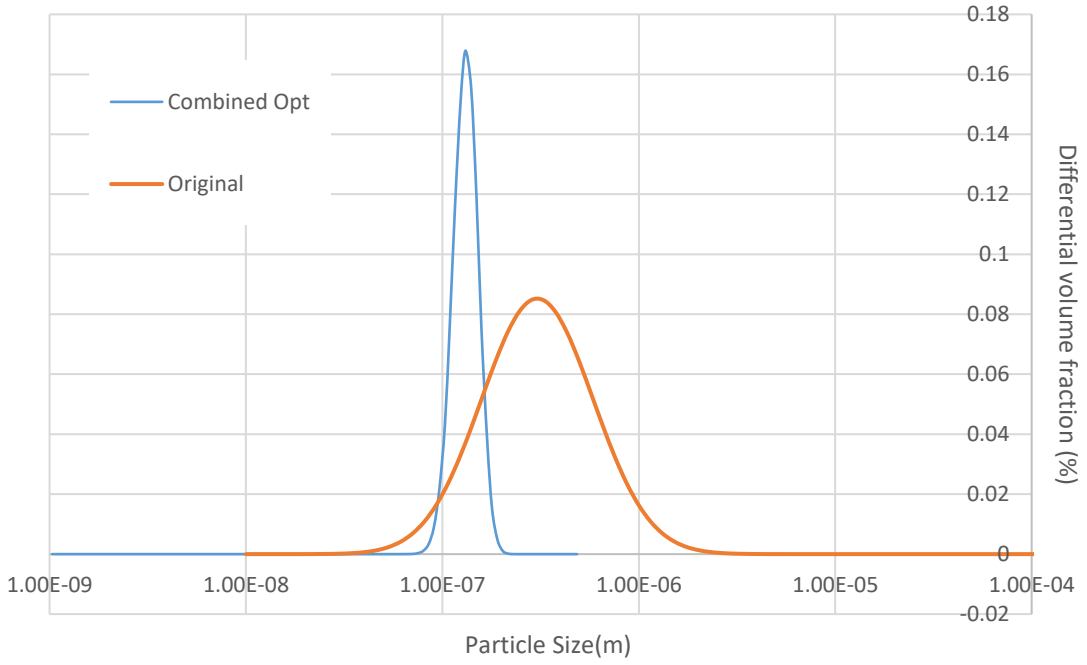

Figure 5.9 Combined parameter and PSD optimisation

From Figure 5.8, it can be observed that the combined optimisation results fall between the original values and the calculated values, demonstrating the effectiveness of the combined optimisation algorithm. In Figure5.9, the PSD distribution is more concentrated compared to the original values and the individually optimised PSD values, proving that the results obtained from combined optimisation are better.

CHAPTER 6. CONCLUSIONS AND RECOMMENDATIONS

This thesis investigated various methods for measuring particle size distribution, both domestically and internationally. After considering multiple factors, it was concluded that the ultrasonic attenuation method is an excellent approach for measuring particle size distribution. Through the study of ultrasonic attenuation mechanisms, various models used in ultrasonic attenuation were examined. The research showed that the ECAH model, which considers comprehensive attenuation mechanisms, is the most suitable. However, it has some limitations, mainly requiring a significant number of physical parameters, which restrict its applicability.

To address this limitation, mathematical optimisation methods were employed to simulate and optimise the unknown physical parameters. Three optimisation algorithms, parallel traversal algorithm, genetic algorithm, and particle swarm algorithm, were utilized. Average particle size of 100nm Silicon dioxide in the water was used in the research. The study encompassed single parameter optimisation, multi-parameter optimisation, PSD optimisation, and combined optimisation. The results demonstrated that the optimisation performed exceptionally well.

In summary, the ultrasonic attenuation method is an effective approach for online measurement of particle size distribution. Optimisation algorithms can accurately and efficiently estimate unknown physical parameters. The combination of optimisation algorithms with ultrasonic attenuation simplifies the use of the ECAH model, enhancing the accuracy of particle size distribution measurements. This makes the ultrasonic attenuation method more widely applicable in the field of particle size measurement.

This method's applicability to different systems and its suitability for calculating unknown parameters are both worth further investigations. The computation time for multi-parameter optimisation is excessively long and requires further optimisation. Additionally, the lack of experimental data prevents further validation of the results.

REFERENCES

ALLEGRA, J. R. & HAWLEY, S. A. 1972. Attenuation of Sound in Suspensions and Emulsions - Theory and Experiments. *Journal of the Acoustical Society of America,* 51**,** 1545-&.

BARITAKI, S., TZANAKAKIS, G. N., ALIFRAGIS, J., ZAFIROPOULOS, A., TASHMUKHAMEDOV, R. I., TSATSAKIS, A., SHTILMAN, M. I., RIZOS, A. K. & KRAMBOVITIS, E. 2002. Light scattering and in vitro biocompatibility studies of poly (vinyl pyrrolidone) derivatives with amino-acid-dependent groups. *Journal of Biomedical Materials Research Part A,* 63**,** 830-837.

CHALLIS, R. E., POVEY, M. J. W., MATHER, M. L. & HOLMES, A. K. 2005. Ultrasound techniques for characterizing colloidal dispersions. *Reports on Progress in Physics,* 68**,** 1541-1637.

CHEEKE, J. D. N. 2012. Fundamentals and applications of ultrasonic waves. 2nd ed. Boca Raton: CRC Press,.

CHEN, Y. 2007. *Ultrasonic wave propagation in concentrated emulsions and encapsulated emulsions.* University of Nottingham.

CHRISTENSON, H. K. 2013. Two-step crystal nucleation via capillary condensation. *CrystEngComm,* 15**,** 2030-2039.

CHUNSHENG, W., YONGQUAN, L., JING, W., QIDONG, W. & XIANGCAI, M. 1994. Thermodynamic Theory of Nucleation Process. *Journal Of Synthetic Crystals***,** 5.

CORZO, D. M. C., BORISSOVA, A., HAMMOND, R. B., KASHCHIEV, D., ROBERTS, K. J., LEWTAS, K. & MORE, I. 2014. Nucleation mechanism and kinetics from the analysis of polythermal crystallisation data: methyl stearate from kerosene solutions. *CrystEngComm,* 16**,** 974-991.

COSTON, S. D. & GEORGE, N. 1991. Particle sizing by inversion of the optical transform pattern. *Applied optics,* 30**,** 4785-4794.

DAVEY, R. J., SCHROEDER, S. L. & TER HORST, J. H. 2013. Nucleation of organic

crystals—a molecular perspective. *Angewandte Chemie International Edition,* 52**,** 2166-2179.

DICKINSON, E., MA, J. & POVEY, M. J. 1994. Creaming of concentrated oil-in-water emulsions containing xanthan. *Food Hydrocolloids,* 8**,** 481-497.

DRENTH, J. & HAAS, C. 1998. Nucleation in protein crystallization. *Acta Crystallographica Section D: Biological Crystallography,* 54**,** 867-872.

DUKHIN, A. S. 2002. *Ultrasound for Characterizing Colloids Particle Sizing, Zeta Potential Rheology*, Elsevier.

EPSTEIN, P. S. & CARHART, R. R. 1953. The Absorption of Sound in Suspensions and Emulsions .1. Water Fog in Air. *Journal of the Acoustical Society of America,* 25**,** 553-565.

ERDEMIR, D., LEE, A. Y. & MYERSON, A. S. 2009. Nucleation of crystals from solution: classical and two-step models. *Accounts of chemical research,* 42**,** 621-629.

EVANS, J. M. & ATTENBOROUGH, K. 1997. Coupled phase theory for sound propagation in emulsions. *Journal of the Acoustical Society of America,* 102**,** 278-282.

FALOLA, A. A. 2015. *Online measurement and population balance modelling of stirred nano-milling.* Thesis (Ph D), University of Leeds (School of Chemical and Process Engineering).

FOKIN, V. M. & ZANOTTO, E. D. 2000. Crystal nucleation in silicate glasses: the temperature and size dependence of crystal/liquid surface energy. *Journal of non-crystalline solids,* 265**,** 105-112.

FOLDY, L. L. 1945. The Multiple Scattering of Waves .1. General Theory of Isotropic Scattering by Randomly Distributed Scatterers. *Physical Review,* 67**,** 107-119.

GARCıA-RUIZ, J. M. 2003. Nucleation of protein crystals. *Journal of Structural Biology,* 142**,** 22-31.

GAVEZZOTTI, A. 1999. Molecular aggregation of acetic acid in a carbon tetrachloride solution: a molecular dynamics study with a view to crystal nucleation.

Chemistry-a European Journal, 5**,** 567-576.

GIBBS, J. W. 1879. On the equilibrium of heterogeneous substances.

GLIKO, O., NEUMAIER, N., PAN, W., HAASE, I., FISCHER, M., BACHER, A., WEINKAUF, S. & VEKILOV, P. G. 2005. A metastable prerequisite for the growth of lumazine synthase crystals. *Journal of the American Chemical Society,* 127**,** 3433-3438.

GLIKO, O., PAN, W., KATSONIS, P., NEUMAIER, N., GALKIN, O., WEINKAUF, S. & VEKILOV, P. G. 2007. Metastable liquid clusters in super-and undersaturated protein solutions. *The Journal of Physical Chemistry B,* 111**,** 3106-3114.

HEATH, A. R., FAWELL, P. D., BAHRI, P. A. & SWIFT, J. D. 2002. Estimating average particle size by focused beam reflectance measurement (FBRM). *Particle & Particle Systems Characterization: Measurement and Description of Particle Properties and Behavior in Powders and Other Disperse Systems,* 19**,** 84-95.

HEMAR, Y., HERRMANN, N., LEMARECHAL, P., HOCQUART, R. & LEQUEUX, F. 1997. Effective medium model for ultrasonic attenuation due to the thermo-elastic effect in concentrated emulsions. *Journal De Physique Ii,* 7**,** 637-647.

HENGGAO, D. & RONG, Z. 2007. Inspiration on Development and Industrialization of Micro/Nano Science and Technology *Nanotechnology and Precision Engineering,* 5**,** 235-241.

HICKEY, J. & L'HEUREUX, I. 2013. Classical nucleation theory with a radius-dependent surface tension: A two-dimensional lattice-gas automata model. *Physical Review E,* 87**,** 022406.

HIPP, A. K., STORTI, G. & MORBIDELLI, I. 2002. Acoustic characterization of concentrated suspensions and emulsions. 1. Model analysis. *Langmuir,* 18**,** 391-404.

HUANG, L., CAO, H., LIU, Y., YAN, E., FENGLI, H. E. & YIN, D. 2014. Research Progresses of Nucleation Theory of Crystals. *Materials Review*.

HUI, L., XUEFENG, S. & LIZHEN, L. 2014. Comparative between sieving method and microscope

in particle size distribution of aged refuse. *Chinese Journal of Environmental*

Engineering, 4007-4011.

KAM, Z., SHORE, H. & FEHER, G. 1978. On the crystallization of proteins. *Journal of molecular biology,* 123, 539-555.

KENNEDY, J. & EBERHART, R. Particle swarm optimization. Proceedings of ICNN'95-international conference on neural networks, 1995. ieee, 1942-1948.

KIM, S. & KARRILA, S. 1991. Butterworth-Heinemann series in chemical engineering. Boston: Butterworth-Heinemann.

KRISHNAN, R. & LINDQUIST, S. L. 2005. Structural insights into a yeast prion illuminate nucleation and strain diversity. *Nature,* 435, 765.

KUZNETSOV, Y. G., MALKIN, A. J. & MCPHERSON, A. 2001. The liquid protein phase in crystallization: a case study—intact immunoglobulins. *Journal of crystal growth,* 232, 30-39.

LAAKSONEN, A. & NAPARI, I. 2001. Breakdown of the capillarity approximation in binary nucleation: a density functional study. *The Journal of Physical Chemistry B,* 105, 11678-11682.

LANGER, J. 1968. Theory of nucleation rates. *Physical Review Letters,* 21, 973.

LLOYD, P. & BERRY, M. V. 1967. Wave Propagation through an Assembly of Spheres .4. Relations between Different Multiple Scattering Theories. *Proceedings of the Physical Society of London,* 91, 678-&.

LOTHE, J. & POUND, G. M. 1962. Reconsiderations of nucleation theory. *The Journal of Chemical Physics,* 36, 2080-2085.

MAES, D., VORONTSOVA, M. A., POTENZA, M. A., SANVITO, T., SLEUTEL, M., GIGLIO, M. & VEKILOV, P. G. 2015. Do protein crystals nucleate within dense liquid clusters? *Acta Crystallographica Section F: Structural Biology Communications,* 71, 815-822.

MALKIN, A. J. & MCPHERSON, A. 1993. Light scattering investigations of protein and virus crystal growth: ferritin, apoferritin and satellite tobacco mosaic virus. *Journal of crystal growth,* 128, 1232-1235.

MCPHERSON, A. 1997. Recent advances in the microgravity crystallization of biological macromolecules. *Trends in biotechnology,* 15**,** 197.

MIKOL, V., HIRSCH, E. & GIEGé, R. 1989. Monitoring protein crystallization by dynamic light scattering. *FEBS letters,* 258**,** 63-66.

MYERSON, A. S. & GINDE, R. 2002. Crystals, crystal growth, and nucleation. *Handbook of Industrial Crystallization (Second Edition).* Elsevier.

OXTOBY, D. W. 1992. Homogeneous nucleation: theory and experiment. *Journal of Physics: Condensed Matter,* 4**,** 7627.

PETER, T. 1996. Airborne particle analysis for climate studies. *Science,* 273**,** 1352-1353.

PHILLIPS, J. D., KUSHNER, J. P., WHITBY, F. G. & HILL, C. P. 1997. Characterization and crystallization of human uroporphyrinogen decarboxylase. *Protein science,* 6**,** 1343-1346.

ROSENBERGER, F., HOWARD, S., SOWERS, J. & NYCE, T. 1993. Temperature dependence of protein solubility—determination and application to crystallization in X-ray capillaries. *Journal of Crystal Growth,* 129**,** 1-12.

ROSENBERGER, F., VEKILOV, P., MUSCHOL, M. & THOMAS, B. 1996. Nucleation and crystallization of globular proteins—what we know and what is missing. *Journal of Crystal Growth,* 168**,** 1-27.

SARIDAKIS, E. E., SHAW STEWART, P. D., LLOYD, L. F. & BLOW, D. M. 1994. Phase diagram and dilution experiments in the crystallization of carboxypeptidase G2. *Acta Crystallographica Section D: Biological Crystallography,* 50**,** 293-297.

SAVAGE, J. & DINSMORE, A. 2009. Experimental evidence for two-step nucleation in colloidal crystallization. *Physical review letters,* 102**,** 198302.

SHUKLA, A., PRAKASH, A. & ROHANI, S. 2010. Particle size monitoring in dense suspension using ultrasound with an improved model accounting for low-angle scattering. *AIChE journal,* 56**,** 2825-2837.

SONG MEIFENG , L. D., WU ZHIMIN, HUA ZEZHAO 2004. Study on Nucleation and Growth Mechanism of Snow Crystal. *Refrigeration Journal,* 25**,** 5.

SPELT, P. D., NORATO, M. A., SANGANI, A. S. & TAVLARIDES, L. L. 1999. Determination of particle size distributions from acoustic wave propagation measurements. *Physics of Fluids,* 11**,** 1065-1080.

SULLO, A. & NORTON, I. 2016. Food Colloids and Emulsions.

TEN WOLDE, P. R. & FRENKEL, D. 1997. Enhancement of protein crystal nucleation by critical density fluctuations. *Science,* 277**,** 1975-1978.

TURNBULL, D. 1950. Kinetics of heterogeneous nucleation. *The Journal of Chemical Physics,* 18**,** 198-203.

VEKILOV, P. G. 2004. Dense liquid precursor for the nucleation of ordered solid phases from solution. *Crystal Growth & Design,* 4**,** 671-685.

VEKILOV, P. G. 2005. Two-step mechanism for the nucleation of crystals from solution. *Journal of crystal growth,* 275**,** 65-76.

VEKILOV, P. G. 2010a. Nucleation. *Crystal growth & design,* 10**,** 5007-5019.

VEKILOV, P. G. 2010b. The two-step mechanism of nucleation of crystals in solution. *Nanoscale,* 2**,** 2346-2357.

WATERMAN, P. C. & TRUELL, R. 1961. Multiple Scattering of Waves. *Journal of Mathematical Physics,* 2**,** 512-&.

WEETALL, H. H. & GAIGALAS, A. K. 1993. A method for the assay of hydrolytic enzymes using dynamic light scattering. *Applied biochemistry and biotechnology,* 41**,** 139-144.

WEN-KAI, L., YU-XIN, W., ZHI-MIN, H., FAN RONG & JUN-FU, L. 2007. Measurement Results Comparison Between Laser Particle Analyzer and Sieving Method in Particle Size Distribution. *China Powder Science and Technology,* 13**,** 10-13.

WENJUN, L., ERWEI, S., YANQING, Z., ZHIZHAN, C. & ZHIWEI, Y. 2000. Nucleating Mechanism of Oxide Crystal and Its Particle Size *JOURNAL OF INORGANIC MATERIALS,* 15**,** 9.

WHITLEY, D. 1994. A genetic algorithm tutorial. *Statistics and computing,* 4**,** 65-85.

YANG LIU , C. Q.-Y., YIN ZHOU-LAN , ZHANG LI-CHUAN 2008. Study on Primary

Nucleation of Supersaturated Sodium Aluminate Solution by Induction Period. *Nonferrous Metals(Extractive Metallurgy)*, 3.

YAU, S.-T. & VEKILOV, P. G. 2000. Quasi-planar nucleus structure in apoferritin crystallization. *Nature,* 406, 494.

YU, A. & STANDISH, N. 1990. A study of particle size distributions. *Powder Technology,* 62, 101-118.

ZELENYUK, A., CABALO, J., BAER, T. & MILLER, R. E. 1999. Mass spectrometry of liquid aniline aerosol particles by IR/UV laser irradiation. *Analytical chemistry,* 71, 1802-1808.

ZHENG PINGYOU, Y. J., ZHANG SHUPING, MA YINGHAI, LIU FUORNG 2006. Study of Heat and Mass Transfer Patterns in Evaporative Crystallization Systems. *Science Technology and Engineering,* 6, 4.

ZIEMANN, P. J. & MCMURRY, P. H. 1998. Secondary electron yield measurements as a means for probing organic films on aerosol particles. *Aerosol science and technology,* 28, 77-90.